Cell Reports

Article

MrgprA3-expressing pruriceptors drive pruritogen-induced alloknesis through mechanosensitive Piezo2 channel

Graphical abstract

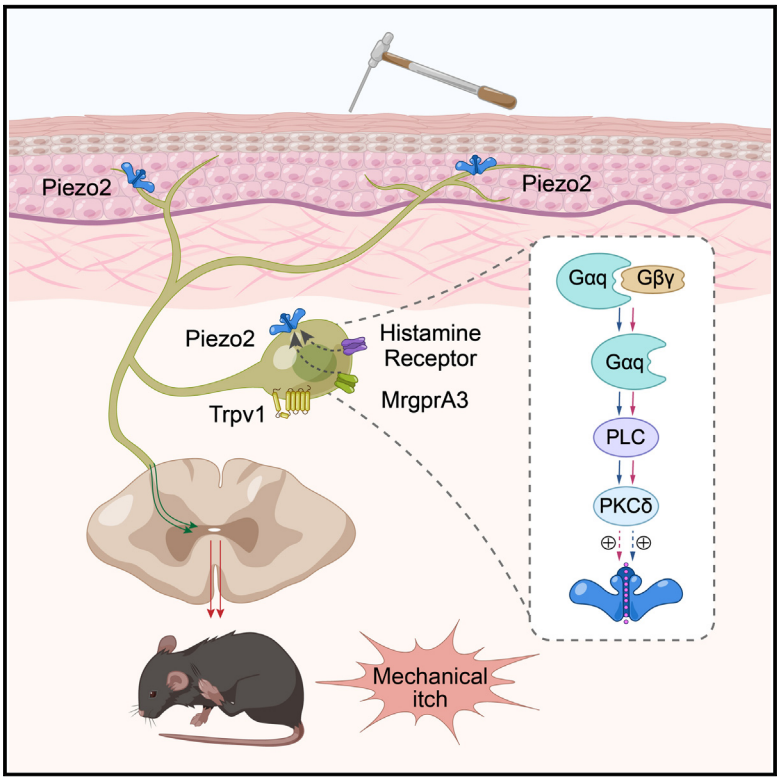

Authors

Ping Lu, Yonghui Zhao, Zili Xie, ..., Brian S. Kim, Jing Feng, Hongzhen Hu

Correspondence

fengjing@simm.ac.cn (J.F.), hongzhen.hu@wustl.edu (H.H.)

In brief

Lu et al. showed that mechanosensitive Piezo2 expressed by the TRPV1$^+$/MrgprA3$^+$ pruriceptors contributes to pruritogen-induced alloknesis. Specifically, their results uncover a pruritogen-activated PLC-PKCδ signaling pathway that sensitizes Piezo2 channel function to produce hypersensitivity in MrgprA3$^+$ pruriceptors in response to mechanical stimulation.

Highlights

- TRPV1$^+$/MrgprA3$^+$ neurons are critical to the initiation of mechanical itch
- TRPV1$^+$/MrgprA3$^+$ neurons are required for pruritogen-induced mechanical itch sensitization
- Piezo2 channel mediates pruritogen-induced mechanical itch sensitization
- Sensitization of Piezo2 by PLC-PKCδ signaling underlies pruritogen-induced alloknesis

Lu et al., 2023, Cell Reports *42*, 112283
April 25, 2023
https://doi.org/10.1016/j.celrep.2023.112283

CellPress

Cell Reports

CellPress
OPEN ACCESS

Article

MrgprA3-expressing pruriceptors drive pruritogen-induced alloknesis through mechanosensitive Piezo2 channel

Ping Lu,[1,2,9] Yonghui Zhao,[1,9] Zili Xie,[1,9] Huan Zhou,[3,4] Xinzhong Dong,[5,6] Gregory F. Wu,[7] Brian S. Kim,[8] Jing Feng,[1,3,4,*] and Hongzhen Hu[1,10,*]

[1]Department of Anesthesiology, The Center for the Study of Itch & Sensory Disorders, Washington University School of Medicine, St. Louis, MO, USA
[2]Dermatology Hospital, Southern Medical University, Guangzhou, China
[3]Center for Neurological and Psychiatric Research and Drug Discovery, Shanghai Institute of Materia Medica, Chinese Academy of Science, Shanghai, China
[4]University of Chinese Academy of Sciences, Beijing, China
[5]The Solomon H. Snyder Department of Neuroscience, Johns Hopkins University School of Medicine, Baltimore, MD 21205, USA
[6]Howard Hughes Medical Institute, Johns Hopkins University School of Medicine, Baltimore, MD 21205, USA
[7]Department of Neurology, Washington University School of Medicine, St. Louis, MO, USA
[8]Kimberly and Eric J. Waldman Department of Dermatology, Icahn School of Medicine at Mount Sinai, New York, NY, USA
[9]These authors contributed equally
[10]Lead contact
*Correspondence: fengjing@simm.ac.cn (J.F.), hongzhen.hu@wustl.edu (H.H.)
https://doi.org/10.1016/j.celrep.2023.112283

SUMMARY

Although touch and itch are coded by distinct neuronal populations, light touch also provokes itch in the presence of exogenous pruritogens, resulting in a phenomenon called alloknesis. However, the cellular and molecular mechanisms underlying the initiation of pruritogen-induced mechanical itch sensitization are poorly understood. Here, we show that intradermal injections of histamine or chloroquine (CQ) provoke alloknesis through activation of TRPV1- and MrgprA3-expressing prurioceptors, and functional ablation of these neurons reverses pruritogen-induced alloknesis. Moreover, genetic ablation of mechanosensitive Piezo2 channel function from MrgprA3-expressing prurioceptors also dampens pruritogen-induced alloknesis. Mechanistically, histamine and CQ sensitize Piezo2 channel function, at least in part, through activation of the phospholipase C (PLC) and protein kinase C-δ (PKCδ) signaling. Collectively, our data find a TRPV1$^+$/MrgprA3$^+$ prurioceptor-Piezo2 signaling axis in the initiation of pruritogen-induced mechanical itch sensitization in the skin.

INTRODUCTION

Alloknesis (or mechanical itch sensitization) is defined as an abnormal sensory state where innocuous mechanical stimuli (such as that from clothing) evoke nocuous itch sensation in the settings of pruritogen stimulation and chronic itch. Although the phenomenon is well known clinically, mouse models of pruritogen-induced mechanical itch were not established until the year of 2012.[1] Recent exciting studies have begun to identify critical spinal cord inhibitory neurons and excitatory neurons in the modulation and transduction of mechanical itch signaling.[2–5] Moreover, alloknesis can also be promoted by a loss of inhibitory Piezo2-Merkel cell signaling as well as inhibitory CD26-mediated dipeptidylpeptidase IV (DPPIV) enzyme activity in the skin.[6,7] However, the cellular and molecular mechanisms mediating mechanical itch in the skin are incompletely understood.

Recent RNA sequencing studies have revealed that a subpopulation of TRPV1-expressing (TRPV1$^+$) neurons express Mas-related G protein-coupled receptor member A3 (MrgprA3) and serve as a direct target for histamine and chloroquine (CQ) to mediate chemical-induced itch sensation in mice.[8,9] Moreover, it was reported that MrgprA3-TRP channel signaling initiates itch sensation but that MrgprA3-P2X3 signaling produces pain sensation, suggesting that MrgprA3 signaling may function as a polymodal signal integrator to allow the diversification of somatosensation.[8,10,11] Interestingly, although *in vivo* electrophysiological recordings showed that MrgprA3$^+$ neurons respond to mechanical stimuli,[12,13] the molecular basis of the mechanosensitivity in the MrgprA3$^+$ neurons remains unknown, and the physiological/pathological relevance of MrgprA3$^+$ neurons in mechanosensation also needs to be determined.

Piezo2 is a bona fide mechanosensitive ion channel and mediates the rapidly adapting (RA) mechanically activated (MA) currents in response to mechanical stimuli in various cell types.[14–18] In addition to its expression in Merkel cells and thickly myelinated slowly adapting type I (SAI) fibers, Piezo2 channel expressed by

thinly myelinated Aδ and unmyelinated C afferents mediates mechanical hypersensitivity in response to tissue inflammation and peripheral nerve injury.[14,19–21] In contrast, whether the Piezo2 channel is involved in chemical itch and/or mechanical itch is not well understood, and the cellular basis of sensory neuron-expressed Piezo2 in the development of itch sensation remains largely unexplored.

Here, we show that TRPV1$^+$/MrgprA3$^+$ neurons are required for mechanical itch induced by both histamine and CQ. Importantly, alloknesis-associated mechanohypersensitivity in the TRPV1$^+$/MrgprA3$^+$ neurons relies on the sensitization of the Piezo2 channel via Gαq/phospholipase C (PLC)/protein kinase C-δ (PKCδ) signaling downstream of the activation of histamine receptors and MrgprA3, initiating mechanical itch but not acute chemical itch. Collectively, our data demonstrate that MrgprA3$^+$ prurioceptor-Piezo2 signaling is essential to the generation of pruritogen-induced alloknesis.

RESULTS

Chemogenetic activation of TRPV1$^+$ neurons promotes mechanical itch

Large-scale single-cell RNA sequencing revealed three distinct subtypes of mechanosensitive nociceptive DRG neurons innervating the skin: the non-peptidergic polymodal C fibers expressing MrgprD, the peptidergic polymodal C fibers expressing TRPV1, and the low-threshold mechanosensitive C fibers (C-LTMRs) expressing tyrosine hydroxylase (TH) and vesicular glutamate transporter type 3 (VGlut3).[22] To determine the classes of DRG neurons involved in the generation of mechanical itch, we first investigated if chemogenetic stimulation of distinct DRG subpopulations is sufficient to cause mechanical itch. We generated *Trpv1-hM3Dq*, *Th-hM3Dq*, and *MrgprD-hM3Dq* mice by crossing *Trpv1^{Cre}*, *Th^{CreER}*, and *MrgprD^{CreERT}* with *Rosa26$^{CAG\text{-}ds\text{-}hM3Dq}$* mice, respectively. Intradermal injections of the DREADD agonist clozapine N-oxide (CNO) into the nape of neck induced a robust, spontaneous scratching response (acute chemical itch) in the *Cre*$^+$, but not *Cre*$^-$, *Trpv1-hM3Dq* mice (Figures S1A and S1B). Interestingly, 30 min after the CNO injection, when the spontaneous scratching subdued, a light touch stimulation delivered by a 0.7 mN von Frey hair filament induced significantly increased mechanical itch in the *Cre*$^+$ *Trpv1-hM3Dq* mice when compared with their *Cre*$^-$ littermates (Figure 1A), recapitulating the alloknesis phenotype produced by intradermal injections of pruritogens.[1]

To ensure that the chemogenetic activation-induced scratching behavior in mice is not a nociceptive response, we employed the well-established cheek model, which provides a behavioral differentiation between itch and pain in mice. As expected, intradermal injections of CNO in the cheek induced a robust scratching response in the *Cre*$^+$, but not *Cre*$^-$, *Trpv1-hM3Dq* mice (Figure S1C), while there were no differences in wiping behavior between these two groups (Figure S1D), suggesting that chemogenetic activation of TRPV1$^+$ neurons evokes alloknesis, but not allodynia, in mice. On the other hand, after Cre induction by intraperitoneal injections of tamoxifen for 5 consecutive days, neither *Cre*$^+$ *Th-hM3Dq* nor *MrgprD-hM3Dq* mice showed increased mechanical itch in response to CNO treatment when compared with their respective *Cre*$^-$ littermates (Figures 1B and 1C). Collectively, these results demonstrate that TRPV1-lineage neurons, but not mechanosensitive primary afferents expressing Th or MrgprD, are critically involved in the initiation of mechanical itch.

Chemically or genetically induced ablation of TRPV1$^+$ neurons reduces mechanical itch provoked by histamine or CQ

Although TRPV1$^+$ DRG neurons are defined as a specific subset of peptidergic sensory neurons in adult mice, which is not overlapped with other C-LTMR markers such as VGlut3/TH and MrgprD,[23,24] TRPV1 mRNA is transiently expressed in a wide range of DRG neurons during development, including TRPV1$^+$ and TRPM8-expressing neurons as well as MrgprD-expressing neurons. Thus, there is a possibility that the *Trpv1^{Cre}* line may non-selectively label other TRPV1$^-$ nociceptive DRG neurons in adult mice. To further confirm the role of TRPV1$^+$ neurons in the generation of pruritogen-induced alloknesis, we employed loss-of-function studies either by ablating TRPV1$^+$ nociceptors with intradermal injections of a super potent TRPV1 ligand resiniferatoxin (RTX) to wild type (WT) mice or by ablating TRPV1-lineage nociceptors with intraperitoneal injections of diphtheria toxin (DTX) to the *Trpv1^{Cre}*; *ROSA26^{DTR}* mice.

The ablation efficiency of TRPV1$^+$ DRG neurons was confirmed by significantly reduced thermal pain behavior in mice and reduced calcium influx in response to CQ and capsaicin in live-cell calcium imaging assays using isolated DRG neurons (Figures S2A–S2D). As expected, acute scratching evoked by either histamine or CQ was significantly reduced in RTX-treated mice and DTX-treated *Cre*$^+$ *Trpv1^{Cre}*; *ROSA26^{DTR}* mice when compared with their respective controls (Figures S3A–S3D). Surprisingly, in contrast to a previous study showing that CQ did not evoke alloknesis at a concentration of 200 nmol/10 μL,[1] intradermal injections of CQ evoked mechanical itch in a bell-shaped manner, with the peak effect produced by a concentration of 50 nmol/30 μL (Figures S4A–S4D), suggesting that higher concentrations of CQ may lead to an inhibition and/or desensitization of alloknesis. Moreover, both histamine- and CQ-induced mechanical itch was markedly reduced in the RTX-treated WT mice and DTX-treated *Cre*$^+$ *Trpv1^{Cre}*; *ROSA26^{DTR}* mice when compared with their respective controls (Figures 1D–1G), while silencing the TRPV1$^+$ neurons by selective delivery of a charged membrane-impermeable sodium channel blocker lidocaine N-ethyl-lidocaine (QX-314)[25] plus CQ also significantly reduced CQ- and histamine-induced mechanical itch (Figures S5A and S5B). Taken together, these results suggest that TRPV1$^+$ C fibers are necessary and sufficient to produce pruritogen-induced mechanical itch.

MrgprA3$^+$ pruriceptors mediate mechanical itch

A subpopulation of TRPV1$^+$ and histamine receptor$^+$ neurons express MrgprA3 and play important roles in histamine- and CQ-induced itch sensation.[8,26,27] However, whether MrgprA3$^+$ prurioceptors are involved in the pathogenesis of pruritogen-induced alloknesis remains unknown. To address this

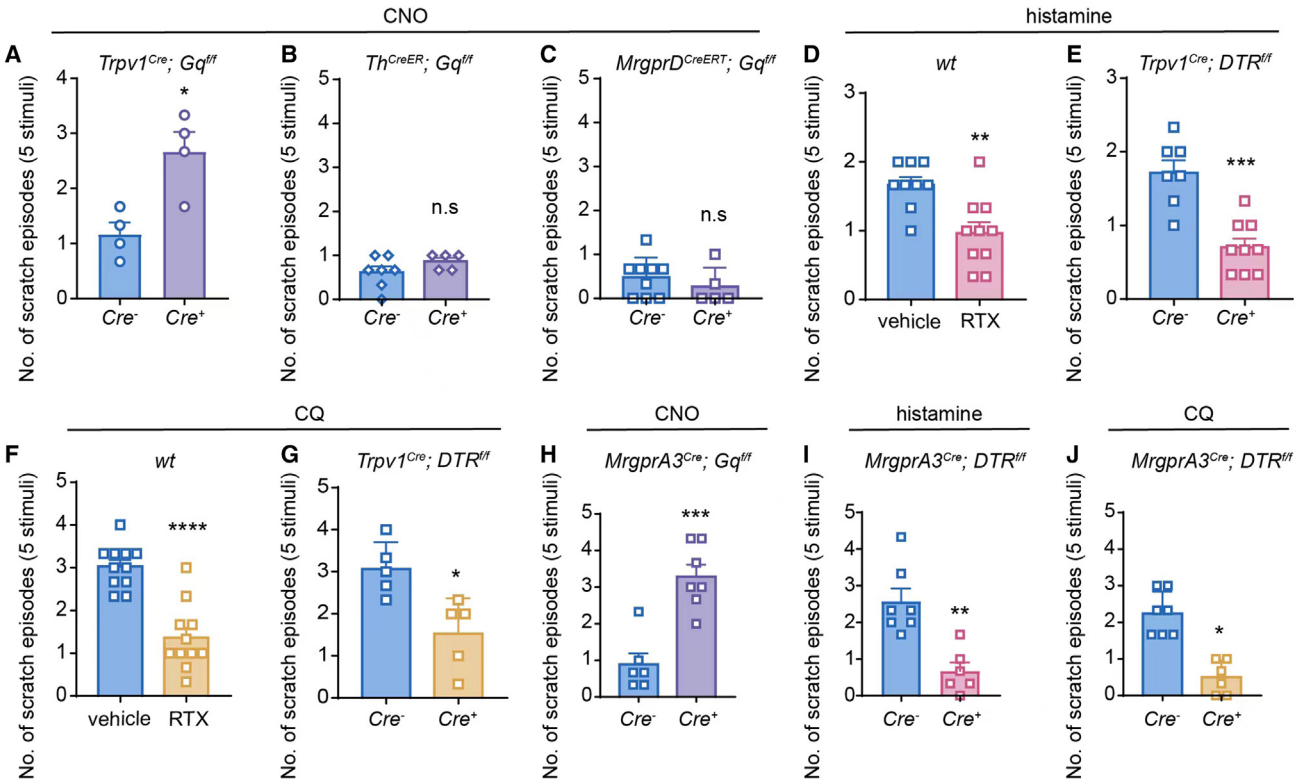

Figure 1. TRPV1$^+$/MrgprA3$^+$ neurons are critically involved in the initiation of mechanical itch

(A) CNO-induced alloknesis scores in *Cre*$^-$ and *Cre*$^+$ *Trpv1-hM3Dq* mice. n = 4 for each group.
(B) CNO-induced alloknesis scores in *Cre*$^-$ (n = 7) and *Cre*$^+$ (n = 5) *Th-hM3Dq* mice.
(C) CNO-induced alloknesis scores in *Cre*$^-$ (n = 9) and *Cre*$^+$ (n = 5) *MrgprD-hM3Dq* mice.
(D) Histamine-induced alloknesis scores in RTX-treated WT mice (n = 10) and vehicle-treated WT mice (n = 9).
(E) Histamine-induced alloknesis scores in *Cre*$^-$ (n = 7) and *Cre*$^+$ (n = 9) *Trpv1-DTR* mice.
(F) CQ-induced alloknesis scores in RTX-treated WT mice (n = 11) and vehicle-treated WT mice (n = 11).
(G) CQ-induced alloknesis scores in *Cre*$^-$ (n = 5) and *Cre*$^+$ (n = 5) *Trpv1-DTR* mice.
(H) CNO-induced alloknesis scores in *Cre*$^-$ (n = 6) and *Cre*$^+$ (n = 7) *MrgprA3-hM3Dq* mice.
(I) Histamine-induced alloknesis scores in *Cre*$^-$ (n = 7) and *Cre*$^+$ (n = 6) *MrgprA3-DTR* mice.
(J) CQ-induced alloknesis scores in *Cre*$^-$ (n = 7) and *Cre*$^+$ (n = 6) *MrgprA3-DTR* mice.
All data are expressed as mean ± SEM. n.s, not significant. *p < 0.05, **p < 0.01, ***p < 0.001, ****p < 0.0001. Unpaired two-tailed Student's t test.

question, we expressed the excitatory Gq-DREADD in the MrgprA3$^+$ neurons by crossing *MrgprA3*$^{GFP\text{-}Cre}$ mice with *Rosa26*$^{CAG\text{-}ds\text{-}hM3Dq}$. Intradermal injections of CNO produced robust, spontaneous scratching in the *Cre*$^+$, but not *Cre*$^-$, *MrgprA3-hM3Dq* mice (Figures S6A and S6B), confirming functional expression of hM3Dq in the MrgprA3$^+$ prurioceptors. Interestingly, mechanical itch responses induced by light mechanical stimulations were significantly increased in the *Cre*$^+$, but not the *Cre*$^-$, *MrgprA3-hM3Dq* mice (Figure 1H), recapitulating the mechanical itch response induced by intradermal injections of CQ. Corroborating with the gain-of-function experiments, genetic ablation of the MrgprA3$^+$ neurons resulted in significantly reduced acute chemical itch (Figures S6C–S6E) and mechanical itch (Figure 1I and 1J) in the DTX-treated *MrgprA3*^{cre}*; ROSA26*^{DTR} mice when compared with their littermate controls. Taken together, our results suggest that chemical-induced sensitization of MrgprA3$^+$ neurons is critically involved in the development of pruritogen-induced mechanical itch.

Piezo2, but not TRPA1, is required for pruritogen-induced mechanical itch

Although it is commonly accepted that TRPA1 is expressed by a subset of TRPV1$^+$ nociceptors and acts as a chemosensor mediating both inflammatory and neuropathic pain as well as pruritogen-induced chemical itch, the role of TRPA1 in mechanosensation has been controversial.[28–31] We found that mechanical itch evoked by either histamine or CQ was comparable between the *TRPA1*$^{+/+}$ and *TRPA1*$^{-/-}$ mice (Figure S7), suggesting that TRPA1 is dispensable in the development of pruritogen-induced alloknesis.

Although we have demonstrated that the epithelial Merkel cell-expressing Piezo2 channel modulates mechanical itch through driving Merkel cell-SA1 Aβ signaling,[6] the role of the mechanosensitive Piezo2 channel expressed by the TRPV1$^+$/MrgprA3$^+$ C-type pruriceptors is not known. To address this, we first checked the expression of Piezo2 in TRPV1$^+$/MrgprA3$^+$ neurons using mRNA fluorescent *in situ* hybridization. Indeed, 43.9% of

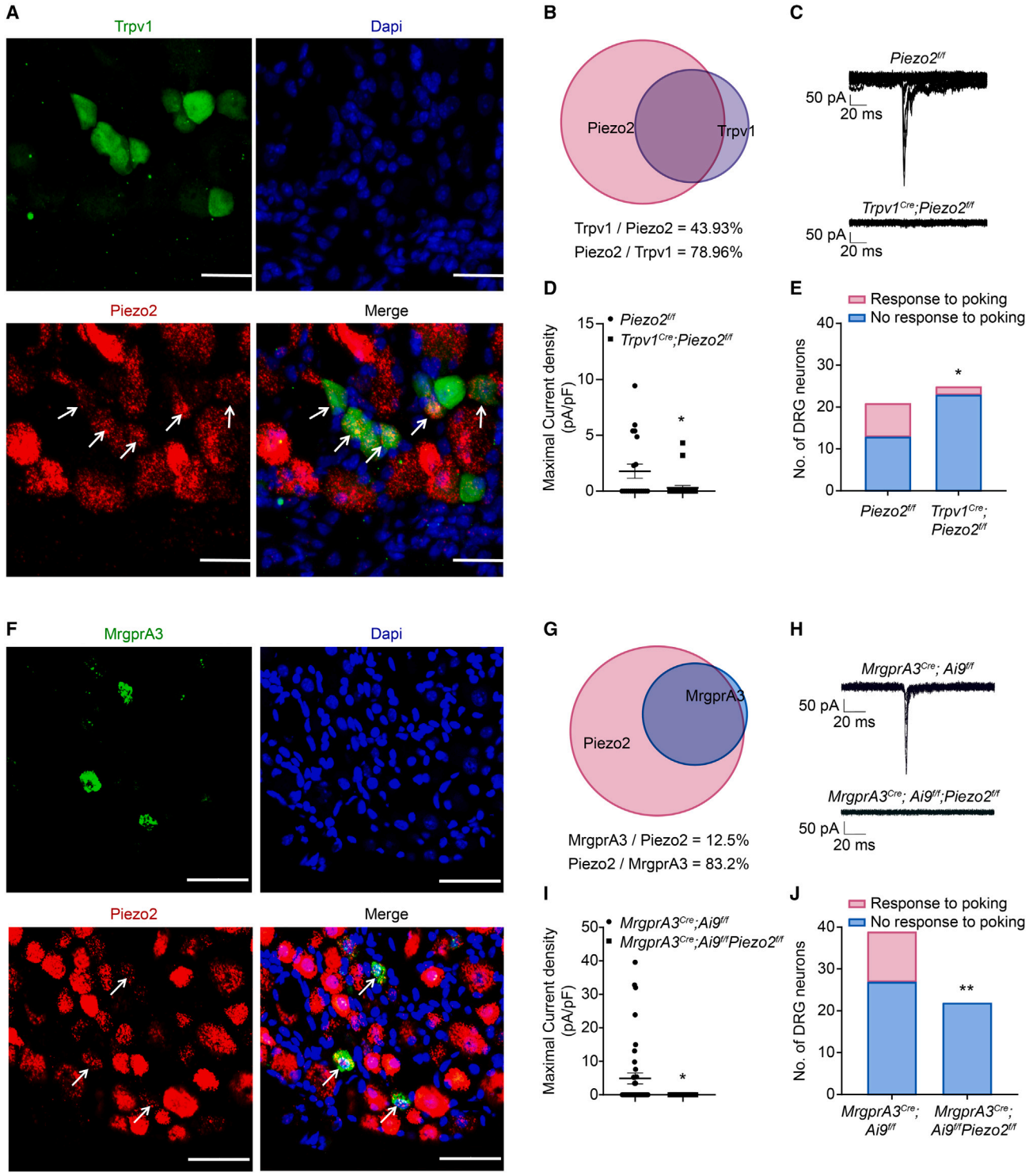

Figure 2. Functional expression of Piezo2 channels in TRPV1$^+$ and MrgprA3$^+$ neurons

(A) Representative images of Piezo2 mRNA transcripts (red) and TRPV1-GFP (green) in DRG neurons isolated from *Trpv1-EGFP* mice. Arrows refer to double-labeled cells. n = 3–5 sections from 3 mice. Scale bar, 50 μm.

(B) The BioVenn diagram illustrates the overlap between TRPV1$^+$ neurons and Piezo2 mRNA$^+$ neurons.

(C) Representative traces of whole-cell MA currents in *Piezo2$^{f/f}$* and *Trpv1^{Cre}; Piezo2$^{f/f}$* neurons.

(D) Current density of whole-cell MA currents in *Piezo2$^{f/f}$* and *Trpv1^{Cre}; Piezo2$^{f/f}$* neurons.

(legend continued on next page)

Piezo2 mRNA-expressing neurons overlapped with the TRPV1-GFP signal and 79.0% of TRPV1-GFP$^+$ neurons expressed Piezo2 mRNA transcripts (Figures 2A and 2B), while 12.5% of Piezo2 mRNA-expressing neurons expressed MrgrpA3-GFP, and more than 80% of MrgprA3-GFP$^+$ neurons displayed Piezo2 mRNA transcripts (Figures 2F and 2G). To determine if Piezo2 is functionally expressed by TRPV1$^+$/MrgprA3$^+$ neurons, we crossed *Trpv1^{Cre}* and *MrgprA3$^{GFP\text{-}cre}$; Ai9$^{f/f}$* mice with *Piezo2$^{f/f}$* mice and performed whole-cell patch-clamp recording. Surprisingly, although the majority of MrgprA3$^+$ neurons express Piezo2 mRNA transcripts, inward whole-cell MA currents were recorded in only 7 out of 20 TRPV1-GFP$^+$ neurons and 12 out of 39 MrgprA3-GFP$^+$ neurons (Figures 2C, 2D, 2H, and 2I), suggesting that the pruriceptor-expressed Piezo2 gene may combine high- and low-translation activities. Of note, only 2 out of 25 TRPV1$^+$ neurons from *Trpv1^{Cre}; Piezo2$^{f/f}$* mice and none of 22 MrgprA3$^+$ neurons from the *MrgprA3^{cre}; Ai9$^{f/f}$; Piezo2$^{f/f}$* mice responded to the same mechanical stimulation protocol (Figures 2E and 2J), suggesting that the Piezo2 channel confers mechanosensitivity to the TRPV1$^+$/MrgprA3$^+$ pruriceptors.

To further investigate whether TRPV1$^+$/MrgprA3$^+$ pruriceptor-expressed Piezo2 is involved in the generation of pruritogen-induced mechanical itch, we injected histamine and CQ into the nape of the neck of the *Trpv1^{Cre}*; *Piezo2$^{f/f}$* mice and *MrgprA3^{cre}; Piezo2$^{f/f}$* mice. Although the acute chemical itch induced by either histamine or CQ was comparable between the *Cre$^-$* and *Cre$^+$ Trpv1^{Cre}*; *Piezo2$^{f/f}$* mice and *MrgprA3^{cre}; Piezo2$^{f/f}$* mice (Figures 3A, 3C, 3E, and 3G), alloknesis scores were markedly reduced in the *Cre$^+$* mice when compared with that in their respective *Cre$^-$* littermates (Figures 3B, 3D, 3F, and 3H), suggesting that Piezo2 is a critical downstream mediator of MrgprA3 signaling in the generation of mechanical itch, but not acute chemical itch, in response to pruritogens in the TRPV1$^+$/MrgprA3$^+$ pruriceptors.

PLC-PKCδ signaling sensitizes Piezo2 to mediate pruritogen-induced mechanical itch

Prior studies demonstrated that increased levels of inflammatory mediators in the inflamed or injured tissues sensitize Piezo2 function, leading to enhanced mechanical hypersensitivity,[14,19,21] which involves multiple intracellular signaling pathways.[20,32,33] Corroborating these findings, both CQ and histamine significantly increased the MA current density in tdTomato$^+$ DRG neurons from the *Cre$^+$ MrgprA3^{cre}; Ai9$^{f/f}$* mice compared with vehicles (Figures 4A and 4B), suggesting that pruritogens sensitize Piezo2 function in the MrgprA3$^+$ pruriceptors.

MrgprA3 and histamine receptors could be dissociated into $G_{\alpha q/11}$ and $G_{\beta\gamma}$ subunits, mediating noxious sensation through coupling to downstream ion channels. To determine the signaling pathways involved in Piezo2 sensitization, we first employed gallein, a small-molecule inhibitor of $G_{\beta\gamma}$ that has been shown to mediate TRPA1-dependent chemical itch.[34,35] Surprisingly, pretreatment of gallein blocked neither the chemical itch nor the mechanical itch induced by CQ or histamine (Figure S8).

On the other hand, it was also reported that CQ-induced spontaneous scratching and neuronal activities were abolished in the PLCβ3 knockout mice.[36] To test whether PLC signaling contributes to MrpgrA3$^+$ neuron sensitization in mechanical itch, we pretreated WT mice with the PLC inhibitor U73122 and the PLC agonist m-3M3FBS. U73122 significantly reduced histamine- and CQ-evoked mechanical itch (Figures 4C and 4D), while application of m-3M3FBS alone was sufficient to promote mechanical itch (Figure 4E). Consistent with these behavioral observations, 3M3FBS also significantly increased both Piezo2 current density and the percentage of mechanosensitive MrgprA3$^+$ DRG neurons (Figures 4F and 4G), suggesting that PLC signaling is necessary and sufficient to promote mechanical itch.

Upon activation, PLC hydrolyzes phosphatidylinositol 4,5-bisphosphate (PIP2) into inositol 1,4,5-trisphosphate (IP3) and 1,2-diacylglycerol (DAG). While IP3 is critical to intracellular Ca^{2+} mobilization, the main effect of DAG is to activate the PKC enzyme, and phospho-PKC (p-PKC) represents a sensitive biomarker of neuronal activity.[37–39] Indeed, immunofluorescent staining and western blot revealed an increased p-PKC protein expression in response to histamine- or CQ-induced activation of the MrgprA3$^+$ neurons, which was further blocked by U73122, but not gallein (Figures 4H–4K and S10), indicating that PLC-PKC signaling is tightly correlated with pruritogen-induced sensitization of the MrgprA3$^+$ neurons. Of note, the family of serine/threonine kinases comprises 11 PKC isoforms encoded by 9 genes.[40] To determine the PKC isoforms involved in MrgprA3-dependent alloknesis, we first reanalyzed the single-cell RNA sequencing (RNA-seq) data of DRG neurons reported by Xing et al., showing that the PKCδ gene is the highest expressed PKC isoform in MrgprA3$^+$ neurons (Figure S9A),[27] which was also shown in our single-cell qRT-PCR data (Figure S9B). To determine the functional role of PKCδ in mechanical itch, we genetically ablated PKCδ from the MrgprA3$^+$ neurons by crossing the *MrgprA3^{cre}* mice with *PKCδ$^{f/f}$* mice. Interestingly, although pruritogen-induced acute chemical itch was comparable, mechanical itch evoked by CQ or histamine was significantly reduced in the *PKCδ^{cko}* mice when compared with their littermate controls (Figures 4L–4O). Taken together, our data demonstrate that intracellular PLC-PKCδ-Piezo2 signaling contributes to the enhanced mechanosensitivity of the MrgprA3$^+$ neurons in pruritogen-induced mechanical itch sensitization.

(E) Summarized data of the percentage of mechanosensitive and mechanoinsensitive DRG neurons recorded in (D).
(F) Representative images of Piezo2 mRNA transcripts (red) and MrgprA3-GFP (green) in DRG neurons isolated from *MrgprA3$^{GFP\text{-}Cre}$* mice. Arrows refer to double-labeled cells. n = 3–5 sections from 3 mice. Scale bar, 50 μm.
(G) The BioVenn diagram illustrates the overlap between MrgprA3$^+$ neurons and Piezo2 mRNA$^+$ neurons.
(H) Representative traces of whole-cell MA currents in *MrgprA3^{cre}; Ai9$^{f/f}$* and *MrgprA3^{cre}; Ai9$^{f/f}$; Piezo2$^{f/f}$* neurons.
(I) Current density of whole-cell currents in *MrgprA3^{cre}; Ai9$^{f/f}$* and *MrgprA3^{cre}; Ai9$^{f/f}$; Piezo2$^{f/f}$* neurons.
(J) Summarized data of the percentage of mechanosensitive and mechanoinsensitive DRG neurons recorded in (I).
*p < 0.05, **p < 0.01. Unpaired two-tailed Student's t test for (D) and (I) and chi-squared test for (E) and (J).

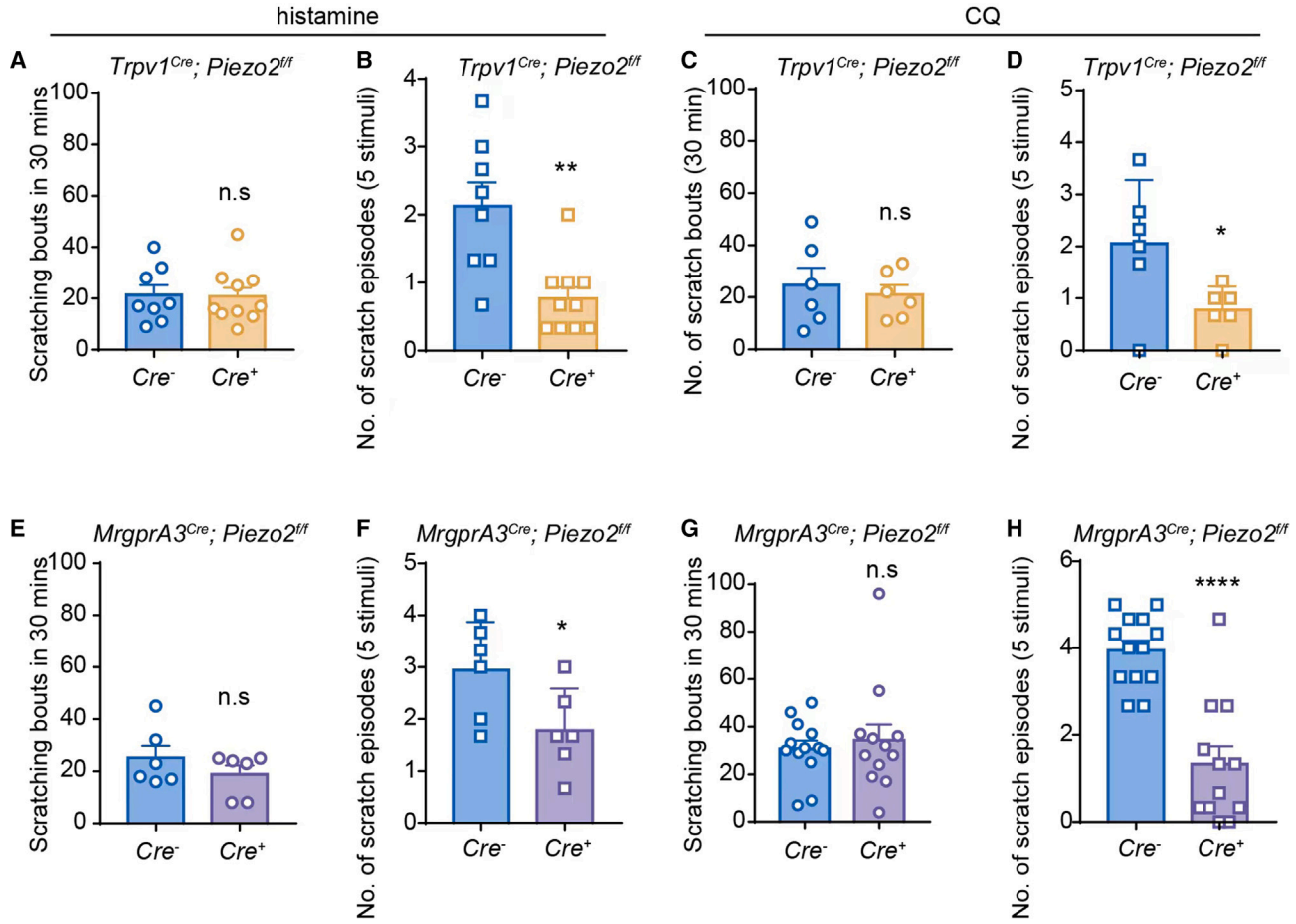

Figure 3. Conditional ablation of Piezo2 function from TRPV1 or MrgprA3 lineage neurons significantly attenuates pruritogen-induced mechanical itch without affecting chemical itch

(A and B) Histamine-induced acute chemical itch (A) and mechanical itch (B) in *Cre*$^{-}$ (n = 8) and *Cre*$^{+}$ (n = 10) *Trpv1*^{Cre}*; Piezo2*$^{f/f}$ mice.

(C and D) CQ-induced acute chemical itch (C) and mechanical itch (D) in *Cre*$^{-}$ (n = 6) and *Cre*$^{+}$ (n = 6) *Trpv1*^{Cre}*; Piezo2*$^{f/f}$ mice.

(E and F) Histamine-induced acute chemical itch (E) and mechanical itch (F) in *Cre*$^{-}$ (n = 6) and *Cre*$^{+}$ (n = 6) *MrgprA3*^{Cre}*; Piezo2*$^{f/f}$ mice.

(G and H) CQ-induced acute chemical itch (G) and mechanical itch (H) in *Cre*$^{-}$ (n = 13) and *Cre*$^{+}$ (n = 12) *MrgprA3*^{Cre}*; Piezo2*$^{f/f}$ mice.

All data are expressed as mean ± SEM. n.s, not significant. *p < 0.05, **p < 0.01, ****p < 0.0001. Unpaired two-tailed Student's t test.

DISCUSSION

Mechanical itch (alloknesis) is an exaggerated itch sensation elicited by innocuous mechanical stimuli, especially in the presence of exogenous pruritogens or in the setting of chronic itch. Although alloknesis was first described 30 years ago,[41,42] the molecular and cellular mechanisms underlying pruritogen-induced alloknesis are not well understood. Here, we provided multiple lines of evidence showing that the TRPV1^{+}/MrgprA3^{+} pruriceptors mediate mechanical itch following administration of CQ or histamine, which requires the function of the mechanosensitive Piezo2 channel. We further demonstrated that intracellular PLC-PKCδ signaling induced by CQ or histamine sensitizes Piezo2 channel function to produce mechanical itch (Figure S11). Our results place the TRPV1^{+}/MrgprA3^{+} pruriceptors-Piezo2 signaling axis at the center of the mechanical itch signaling pathway driven by exogenously applied pruritogens.

Previous studies have shown multiple forms of mechanical itch under both physiological and pathological conditions. For instance, Ucn3-expressing excitatory interneurons as well as the neuropeptide Y1 receptor-expressing excitatory interneurons in the spinal cord are required for the transmission of mechanical itch occurring in specific locations,[2,5] i.e., skin areas behind the ears. Interestingly, the Ucn3^{+} neurons receive inputs from TLR5^{+} Aβ LTMRs, which also express NF200 and contribute to the generation of touch and mechanical allodynia.[5,25] In contrast to the excitatory role of TLR5^{+} Aβ LTMRs, our recent study showed that inhibitory inputs from Piezo2-expressing Merkel cells and innervating SAI-Aβ LTMRs suppress touch-evoked mechanical itch,[6] suggesting that subpopulations of NF200^{+} Aβ fibers have distinct roles in mechanical itch signaling. Besides potential roles of Aβ LTMR subsets in mechanical itch, alloknesis is also associated with chronic skin inflammation such as that in mouse models of experimental

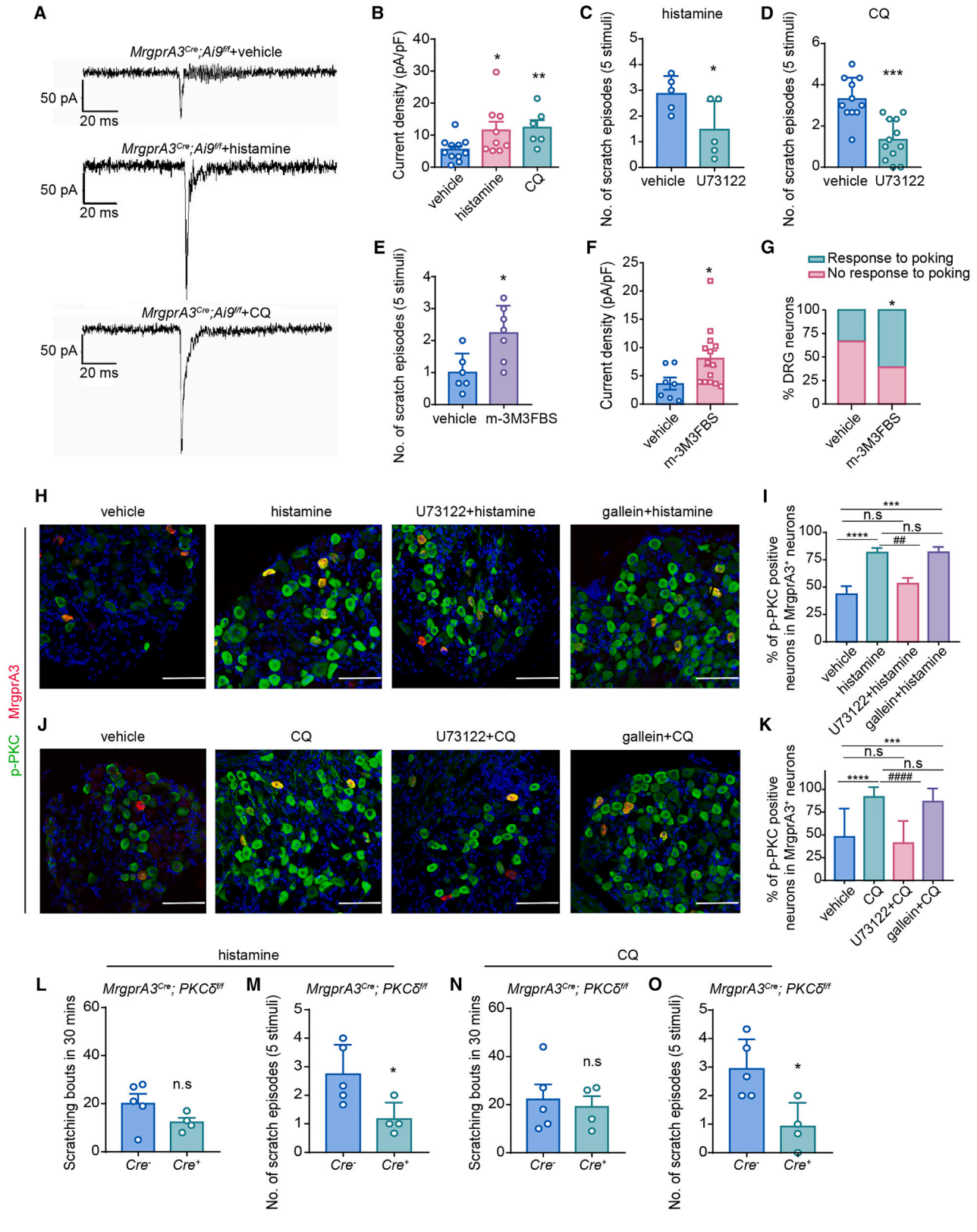

(legend on next page)

dry skin and imiquimod-induced psoriasis as well as exogenously applied pruritogens such as histamine and endomorphins,[1,7,43] which is mainly dependent on the abnormal activities of C pruriceptors, implicating a potential role of C-LTMRs in the development of mechanical itch sensitization. Indeed, C-LTMRs expressing VGlut3/TH and MrgprD were shown to play important roles in mechanical hypersensitivity. For example, VGlut3$^+$/TH$^+$ C-LTMRs mediate mechanical allodynia in the setting of neuropathic pain, while activation of MrgprD$^+$ neurons evokes both acute itch and chronic itch associated with allergic contact dermatitis (ACD) in mice.[12,44–47] However, our genetic studies showed that chemogenetic activation of MrgprD$^+$ and VGlut3$^+$/TH$^+$ neurons does not evoke mechanical itch, suggesting that MrgprD$^+$ non-peptidergic C polymodal nociceptors and VGlut3$^+$/TH$^+$ C-LTMRs are unlikely major players in pruritogen-induced mechanical itch in mice. Interestingly, a recent study demonstrated that the VGlut3-lineage neurons mediate spinal inhibition of pruritogen-evoked chemical itch,[48] suggesting distinct roles of C-LTMRs in itch modulation.

It was recently reported that a subset of itch-sensing, neuron-expressing neuropeptide genes, somatostatin (Sst) and natriuretic polypeptide precursor B (Nppb), are critically involved in the development of mechanical itch. Specifically, Piezo1-expressing pruriceptors respond to histamine primarily through the Sst$^+$Nppb$^+$ neurons to promote mechanical itch and itch sensitization.[49] Of note, Piezo2 was found to be expressed in a smaller percentage of Sst$^+$Nppb$^+$ neurons, while Piezo1 does not overlap with MrgprA3. This distribution pattern suggests that both Piezo1 and Piezo2 are critical mediators for mechanical itch sensitization through conferring mechanical sensitivity to distinct subpopulations of mechanosensitive pruriceptors.

Various ion channels downstream of GPCR signaling pathways contribute to distinct pruritogen-induced itch sensation. For instance, histamine elicits acute chemical itch sensation by activating downstream TRPV1 through PLCβ3 and PLA2/lipoxygenase,[24,36,50,51] and CQ evokes TRPA1-dependent acute chemical itch through a signaling mechanism involving MrgprA3-coupled Gβγ signaling but not PLC.[52] Moreover, inhibition of PKCδ significantly decreases histamine-induced acute chemical itch, as histamine treatment produces PKCδ phosphorylation leading to sensitization of the voltage-gated sodium channel Nav1.7 in pruriceptors.[53,54] Interestingly, our results further showed that PLC-PKCδ signaling-mediated sensitization of the MrgprA3$^+$ neuron-expressing Piezo2 channel plays a pivotal role in pruritogen-induced mechanical itch, but not acute chemical itch, revealing a signaling axis of PLC-PKCδ-Piezo2 in mechanical itch initiation, which is also separate from the roles of the EPAC1-Piezo2 and PKA/PKC-Piezo2 signaling axes in mechanical allodynia.[19,33] Of note, although the mechanical itch responses induced by histamine and CQ were significantly attenuated in mice where PKCδ was conditionally ablated in the MrgprA3$^+$ pruriceptors, we also observed high expression levels of Prkca and Prkce in the MrgprA3$^+$ neurons, which is consistent with a recent report.[55] Therefore, we cannot exclude the possibility that other PKC isoforms might also be involved in the pruritogen-induced sensitization of Piezo2 and the promotion of mechanical itch.

In summary, our findings show that activation of TRPV1$^+$/MrgprA3$^+$ DRG neurons mediates pruritogen-induced mechanical itch by sensitizing the mechanosensitive Piezo2 channel through PLC-PKCδ signaling in the skin. Identification of the MrgprA3$^+$ C pruriceptors in mediating the pruritogen-induced mechanical itch highlights the importance of this small subset of TRPV1$^+$ neurons in the generation of both mechanically stimulated and non-evoked chemical itch not only to the MrgprA3 receptor ligand CQ but also to other pruritogens such as histamine. Our data may also offer a therapeutic target for treating chronic itch.

Limitations of the study

There are a few limitations in this study: first, although the single-cell RT-PCR data in the study showed that Prkcd is the predominant protein kinase in MrgprA3$^+$ neurons, we could not exclude

Figure 4. PLC-PKCδ signaling is critically involved in pruritogen-induced sensitization of mechanosensitive pruriceptors and mechanical itch

(A) Representative whole-cell MA current traces elicited by mechanical indentation on DRG neurons isolated from *MrgprA3^{cre}; Ai9$^{f/f}$* mice perfused with vehicle, histamine, or CQ, respectively.

(B) Summarized data of the current density of mechanosensitive MrgprA3$^+$ neurons in response to vehicle (n = 11), histamine (n = 9), and CQ (n = 6).

(C and D) Histamine-induced (C) and CQ-induced (D) alloknesis scores in mice treated with vehicle or PLC inhibitor U73122. n = 5 mice for each group in (C), n = 11 vehicle-treated and n = 12 U73122-treated mice in (D).

(E) m-3M3FBS-induced alloknesis score in WT mice. n = 6 for vehicle-treated and n = 7 for m-3M3FBS-treated mice.

(F) Current density of whole-cell MA currents in the presence of vehicle and 1 μM m-3M3FBS in neurons isolated from *MrgprA3^{cre};Ai9$^{f/f}$* mice.

(G) Bar graph summarized the percentage of mechanosensitive DRG neurons in presence of vehicle and 1 μM m-3M3FBS.

(H) Representative images of MrgprA3 mRNA transcripts (red) and p-PKC (green) staining in DRG neurons isolated from WT mice treated with vehicle, histamine, U73122 + histamine, and gallein + histamine, respectively. Scale bar, 50 μm.

(I) Quantification of the number of p-PKC-expressing cells in MrgprA3$^+$ neurons in response to different treatments in (H). n = 3–5 sections from 3 mice for each group.

(J) Representative images of MrgprA3 mRNA transcripts (red) and p-PKC (green) staining in DRG neurons isolated from WT mice treated with vehicle, CQ, U73122 + CQ, and gallein + CQ, respectively. Scale bar, 50 μm.

(K) Quantification of the number of p-PKC-expressing cells in MrgprA3$^+$ neurons in response to different treatments in (J). n = 3–5 sections from 3 mice for each group. All scale bars, 100 μm.

(L and M) Histamine-induced acute chemical itch (L) and mechanical itch (M) in *Cre*$^-$ (n = 5) and *Cre*$^+$ (n = 4) *MrgprA3^{Cre}; PKCδ$^{f/f}$* mice.

(N and O) CQ-induced acute chemical itch (N) and mechanical itch (O) in *Cre*$^-$ (n = 5) and *Cre*$^+$ (n = 4) *MrgprA3^{Cre}; PKCδ$^{f/f}$* mice.

Data are expressed as mean ± SEM. n.s, not significant. *p < 0.05, **p < 0.01, ***p < 0.001, ****p < 0.0001, ##p < 0.01, ####p < 0.0001. Unpaired two-tailed Student's t test in (C)–(F) and (L)–(O), chi-squared test for (G), and one-way ANOVA in (B), (I), and (K).

the possibility that other PKC isoforms and/or other signaling pathways might also be involved in the pruritogen-induced sensitization of Piezo2 and the promotion of mechanical itch. Second, our work employed acute mouse models of pruritogen-induced mechanical itch; future work should be performed to determine whether TRPV1$^+$/MrgprA3$^+$ pruriceptors-Piezo2 signaling is also involved in the development of chronic itch-associated alloknesis. Last, while we showed inhibition of PLC-PKC signaling-mitigated mechanical itch in mice, it is challenging to inhibit the functions of MrgprA3 and Piezo2 because of a lack of specific blockers.

STAR★METHODS

Detailed methods are provided in the online version of this paper and include the following:

- KEY RESOURCES TABLE
- RESOURCE AVAILABILITY
  - Lead contact
  - Materials availability
  - Data and code availability
- EXPERIMENTAL MODEL AND SUBJECT DETAILS
  - Animals
  - Primary mouse DRG neuronal culture
- METHOD DETAILS
  - Pruritogen-induced acute chemical itch
  - Pruritogen-induced alloknesis
  - Drug administration
  - Mouse cheek model
  - Pharmacological silence of sensory fibers in the skin
  - In situ hybridization and immunohistochemistry
  - Tail flick test
  - Chemical ablation of TRPV1$^+$ and MrgprA3$^+$ neurons
  - Mouse DRG neuron cultures
  - Live-cell calcium imaging
  - Whole-cell patch-clamp recordings
  - Western blot analysis
  - Single cell RT-PCR
- QUANTIFICATION AND STATISTICAL ANALYSIS

SUPPLEMENTAL INFORMATION

Supplemental information can be found online at https://doi.org/10.1016/j.celrep.2023.112283.

ACKNOWLEDGMENTS

We thank Dr. Mark Hoon for sharing the Trpv1Cre mice and Dr. Xinzhong Dong for sharing the *MrgprA3*$^{GFP\text{-}Cre}$ mouse line. This work is supported by National Institutes of Health grants R01AA027065, R01AR077183, and R01DK103901 to H.H. and R01NS106289 to G.F.W.

AUTHOR CONTRIBUTIONS

H.H. and J.F. conceived the project and wrote the manuscript. P.L. designed and conducted most of mouse behavioral experiments. P.L. and Y.Z. were responsible for RNAscope and immunostaining. Y.Z. and Z.X. were responsible for patch-clamp recordings. Others assisted with the data analysis and manuscript preparation.

DECLARATION OF INTERESTS

B.S.K. has served as a consultant for AbbVie, Almirall S.A., Amagma, Argenx, Astra Zeneca, Bellus Health, Blueprint Medicines, Boehringer Ingelheim Corporation, Bristol-Myers Squibb, Cara Therapeutics, Daewoong Pharmaceutical, Eli Lilly and Company, Guidepoint Global, Janssen Pharmaceuticals, Incyte Corporation, Kiniksa Pharmaceuticals, LectureLinx, LEO Pharma, Maruho, Novartis, OM Pharma, Pfizer, Sanofi Genzyme, Shaperon, Third Rock Ventures, and Trevi Therapeutics; is a stockholder of Recens Medical and Locus Biosciences; and serves on the scientific advisory boards for Abrax Japan, Granular Therapeutics, Recens Medical, National Eczema Association, *Cell Reports Medicine*, and *Journal of Allergy and Clinical Immunology*. B.S.K. is an inventor on a patent/patent application (WO2017143014A1) held/submitted by Washington University that covers the use of JAK inhibitors for chronic pruritus.

INCLUSION OF DIVERSITY

We support inclusive, diverse, and equitable conduct of research.

Received: May 27, 2022
Revised: January 29, 2023
Accepted: March 3, 2023
Published: March 22, 2023

REFERENCES

1. Akiyama, T., Carstens, M.I., Ikoma, A., Cevikbas, F., Steinhoff, M., and Carstens, E. (2012). Mouse model of touch-evoked itch (alloknesis). J. Invest. Dermatol. *132*, 1886–1891. https://doi.org/10.1038/jid.2012.52.
2. Acton,D.,Ren,X.,DiCostanzo,S.,Dalet,A.,Bourane,S.,Bertocchi,I.,Eva,C.,and Goulding,M.(2019).SpinalneuropeptideY1receptor-expressingneuronsformanessentialexcitatorypathwayformechanicalitch.CellRep.*28*,625–639.e6. https://doi.org/10.1016/j.celrep.2019.06.033.
3. Bourane, S., Duan, B., Koch, S.C., Dalet, A., Britz, O., Garcia-Campmany, L., Kim, E., Cheng, L., Ghosh, A., Ma, Q., and Goulding, M. (2015). Gate control of mechanical itch by a subpopulation of spinal cord interneurons. Science *350*, 550–554. https://doi.org/10.1126/science.aac8653.
4. Chen, S., Gao, X.F., Zhou, Y., Liu, B.L., Liu, X.Y., Zhang, Y., Barry, D.M., Liu, K., Jiao, Y., Bardoni, R., et al. (2020). A spinal neural circuitry for converting touch to itch sensation. Nat. Commun. *11*, 5074. https://doi.org/10.1038/s41467-020-18895-7.
5. Pan, H., Fatima, M., Li, A., Lee, H., Cai, W., Horwitz, L., Hor, C.C., Zaher, N., Cin, M., Slade, H., et al. (2019). Identification of a spinal circuit for mechanical and persistent spontaneous itch. Neuron *103*, 1135–1149.e6. https://doi.org/10.1016/j.neuron.2019.06.016.
6. Feng, J., Luo, J., Yang, P., Du, J., Kim, B.S., and Hu, H. (2018). Piezo2 channel-Merkel cell signaling modulates the conversion of touch to itch. Science *360*, 530–533. https://doi.org/10.1126/science.aar5703.
7. Komiya, E., Tominaga, M., Hatano, R., Kamikubo, Y., Toyama, S., Sakairi, H., Honda, K., Itoh, T., Kamata, Y., Tsurumachi, M., et al. (2022). Peripheral endomorphins drive mechanical alloknesis under the enzymatic control of CD26/DPPIV. J. Allergy Clin. Immunol. *149*, 1085–1096. https://doi.org/10.1016/j.jaci.2021.08.003.
8. Han,L.,Ma,C.,Liu,Q.,Weng,H.J.,Cui,Y.,Tang,Z.,Kim,Y.,Nie,H.,Qu,L.,Patel, K.N., et al. (2013). A subpopulation of nociceptors specifically linked to itch. Nat.Neurosci.*16*,174–182.https://doi.org/10.1038/nn.3289.
9. Solinski, H.J., Kriegbaum, M.C., Tseng, P.Y., Earnest, T.W., Gu, X., Barik, A., Chesler, A.T., and Hoon, M.A. (2019). Nppb neurons are sensors of mast cell-induced itch. Cell Rep. *26*, 3561–3573.e4. https://doi.org/10.1016/j.celrep.2019.02.089.
10. Sharif, B., Ase, A.R., Ribeiro-da-Silva, A., and Séguéla, P. (2020). Differential coding of itch and pain by a subpopulation of primary afferent neurons. Neuron *106*, 940–951.e4. https://doi.org/10.1016/j.neuron.2020.03.021.

11. von Buchholtz, L.J., Ghitani, N., Lam, R.M., Licholai, J.A., Chesler, A.T., and Ryba, N.J.P. (2021). Decoding cellular mechanisms for mechanosensory discrimination. Neuron *109*, 285–298.e5. https://doi.org/10.1016/j.neuron.2020.10.028.

12. Qu, L., Fan, N., Ma, C., Wang, T., Han, L., Fu, K., Wang, Y., Shimada, S.G., Dong, X., and LaMotte, R.H. (2014). Enhanced excitability of MRGPRA3- and MRGPRD-positive nociceptors in a model of inflammatory itch and pain. Brain *137*, 1039–1050. https://doi.org/10.1093/brain/awu007.

13. Feng, J., Zhao, Y., Xie, Z., Zang, K., Sviben, S., Hu, X., Fitzpatrick, J.A.J., Wen, L., Liu, Y., Wang, T., et al. (2022). Miswiring of Merkel cell and pruriceptive C fiber drives the itch-scratch cycle. Sci. Transl. Med. *14*, eabn4819. https://doi.org/10.1126/scitranslmed.abn4819.

14. Murthy, S.E., Loud, M.C., Daou, I., Marshall, K.L., Schwaller, F., Kühnemund, J., Francisco, A.G., Keenan, W.T., Dubin, A.E., Lewin, G.R., and Patapoutian, A. (2018). The mechanosensitive ion channel Piezo2 mediates sensitivity to mechanical pain in mice. Sci. Transl. Med. *10*, eaat9897. https://doi.org/10.1126/scitranslmed.aat9897.

15. Wang, L., Zhou, H., Zhang, M., Liu, W., Deng, T., Zhao, Q., Li, Y., Lei, J., Li, X., and Xiao, B. (2019). Structure and mechanogating of the mammalian tactile channel PIEZO2. Nature *573*, 225–229. https://doi.org/10.1038/s41586-019-1505-8.

16. Woo, S.H., Ranade, S., Weyer, A.D., Dubin, A.E., Baba, Y., Qiu, Z., Petrus, M., Miyamoto, T., Reddy, K., Lumpkin, E.A., et al. (2014). Piezo2 is required for Merkel-cell mechanotransduction. Nature *509*, 622–626. https://doi.org/10.1038/nature13251.

17. Woo, S.H., Lukacs, V., de Nooij, J.C., Zaytseva, D., Criddle, C.R., Francisco, A., Jessell, T.M., Wilkinson, K.A., and Patapoutian, A. (2015). Piezo2 is the principal mechanotransduction channel for proprioception. Nat. Neurosci. *18*, 1756–1762. https://doi.org/10.1038/nn.4162.

18. Marshall, K.L., Saade, D., Ghitani, N., Coombs, A.M., Szczot, M., Keller, J., Ogata, T., Daou, I., Stowers, L.T., Bönnemann, C.G., et al. (2020). PIEZO2 in sensory neurons and urothelial cells coordinates urination. Nature *588*, 290–295. https://doi.org/10.1038/s41586-020-2830-7.

19. Dubin, A.E., Schmidt, M., Mathur, J., Petrus, M.J., Xiao, B., Coste, B., and Patapoutian, A. (2012). Inflammatory signals enhance piezo2-mediated mechanosensitive currents. Cell Rep. *2*, 511–517. https://doi.org/10.1016/j.celrep.2012.07.014.

20. Nencini, S., Morgan, M., Thai, J., Jobling, A.I., Mazzone, S.B., and Ivanusic, J.J. (2021). Piezo2 knockdown inhibits noxious mechanical stimulation and NGF-induced sensitization in A-delta bone afferent neurons. Front. Physiol. *12*, 644929. https://doi.org/10.3389/fphys.2021.644929.

21. Szczot, M., Liljencrantz, J., Ghitani, N., Barik, A., Lam, R., Thompson, J.H., Bharucha-Goebel, D., Saade, D., Necaise, A., Donkervoort, S., et al. (2018). PIEZO2 mediates injury-induced tactile pain in mice and humans. Sci. Transl. Med. *10*, eaat9892. https://doi.org/10.1126/scitranslmed.aat9892.

22. Usoskin, D., Furlan, A., Islam, S., Abdo, H., Lönnerberg, P., Lou, D., Hjerling-Leffler, J., Haeggström, J., Kharchenko, O., Kharchenko, P.V., et al. (2015). Unbiased classification of sensory neuron types by large-scale single-cell RNA sequencing. Nat. Neurosci. *18*, 145–153. https://doi.org/10.1038/nn.3881.

23. Cavanaugh, D.J., Lee, H., Lo, L., Shields, S.D., Zylka, M.J., Basbaum, A.I., and Anderson, D.J. (2009). Distinct subsets of unmyelinated primary sensory fibers mediate behavioral responses to noxious thermal and mechanical stimuli. Proc. Natl. Acad. Sci. USA *106*, 9075–9080. https://doi.org/10.1073/pnas.0901507106.

24. Mishra, S.K., and Hoon, M.A. (2013). The cells and circuitry for itch responses in mice. Science *340*, 968–971. https://doi.org/10.1126/science.1233765.

25. Xu, Z.Z., Kim, Y.H., Bang, S., Zhang, Y., Berta, T., Wang, F., Oh, S.B., and Ji, R.R. (2015). Inhibition of mechanical allodynia in neuropathic pain by TLR5-mediated A-fiber blockade. Nat. Med. *21*, 1326–1331. https://doi.org/10.1038/nm.3978.

26. Wilson, S.R., Nelson, A.M., Batia, L., Morita, T., Estandian, D., Owens, D.M., Lumpkin, E.A., and Bautista, D.M. (2013). The ion channel TRPA1 is required for chronic itch. J. Neurosci. *33*, 9283–9294. https://doi.org/10.1523/jneurosci.5318-12.2013.

27. Xing, Y., Chen, J., Hilley, H., Steele, H., Yang, J., and Han, L. (2020). Molecular signature of pruriceptive MrgprA3(+) neurons. J. Invest. Dermatol. *140*, 2041–2050. https://doi.org/10.1016/j.jid.2020.03.935.

28. Brierley, S.M., Castro, J., Harrington, A.M., Hughes, P.A., Page, A.J., Rychkov, G.Y., and Blackshaw, L.A. (2011). TRPA1 contributes to specific mechanically activated currents and sensory neuron mechanical hypersensitivity. J. Physiol. *589*, 3575–3593. https://doi.org/10.1113/jphysiol.2011.206789.

29. Hossain, M.Z., Ando, H., Unno, S., and Kitagawa, J. (2022). TRPA1s act as chemosensors but not as cold sensors or mechanosensors to trigger the swallowing reflex in rats. Sci. Rep. *12*, 3431. https://doi.org/10.1038/s41598-022-07400-3.

30. Kwan, K.Y., Glazer, J.M., Corey, D.P., Rice, F.L., and Stucky, C.L. (2009). TRPA1 modulates mechanotransduction in cutaneous sensory neurons. J. Neurosci. *29*, 4808–4819. https://doi.org/10.1523/jneurosci.5380-08.2009.

31. Lennertz, R.C., Kossyreva, E.A., Smith, A.K., and Stucky, C.L. (2012). TRPA1 mediates mechanical sensitization in nociceptors during inflammation. PLoS One *7*, e43597. https://doi.org/10.1371/journal.pone.0043597.

32. Del Rosario, J.S., Yudin, Y., Su, S., Hartle, C.M., Mirshahi, T., and Rohacs, T. (2020). Gi-coupled receptor activation potentiates Piezo2 currents via Gβγ. EMBO Rep. *21*, e49124. https://doi.org/10.15252/embr.201949124.

33. Eijkelkamp, N., Linley, J.E., Torres, J.M., Bee, L., Dickenson, A.H., Gringhuis, M., Minett, M.S., Hong, G.S., Lee, E., Oh, U., et al. (2013). A role for Piezo2 in EPAC1-dependent mechanical allodynia. Nat. Commun. *4*, 1682. https://doi.org/10.1038/ncomms2673.

34. Lieu, T., Jayaweera, G., Zhao, P., Poole, D.P., Jensen, D., Grace, M., McIntyre, P., Bron, R., Wilson, Y.M., Krappitz, M., et al. (2014). The bile acid receptor TGR5 activates the TRPA1 channel to induce itch in mice. Gastroenterology *147*, 1417–1428. https://doi.org/10.1053/j.gastro.2014.08.042.

35. Morita, T., McClain, S.P., Batia, L.M., Pellegrino, M., Wilson, S.R., Kienzler, M.A., Lyman, K., Olsen, A.S.B., Wong, J.F., Stucky, C.L., et al. (2015). HTR7 mediates serotonergic acute and chronic itch. Neuron *87*, 124–138. https://doi.org/10.1016/j.neuron.2015.05.044.

36. Imamachi, N., Park, G.H., Lee, H., Anderson, D.J., Simon, M.I., Basbaum, A.I., and Han, S.K. (2009). TRPV1-expressing primary afferents generate behavioral responses to pruritogens via multiple mechanisms. Proc. Natl. Acad. Sci. USA *106*, 11330–11335. https://doi.org/10.1073/pnas.0905605106.

37. Freeley, M., Kelleher, D., and Long, A. (2011). Regulation of Protein Kinase C function by phosphorylation on conserved and non-conserved sites. Cell. Signal. *23*, 753–762. https://doi.org/10.1016/j.cellsig.2010.10.013.

38. Hopper, R.A., Forrest, C.R., Xu, H., Zhong, A., He, W., Rutka, J., Neligan, P., and Pang, C.Y. (2000). Role and mechanism of PKC in ischemic preconditioning of pig skeletal muscle against infarction. Am. J. Physiol. Regul. Integr. Comp. Physiol. *279*, R666–R676. https://doi.org/10.1152/ajpregu.2000.279.2.R666.

39. Misonou, H., Menegola, M., Mohapatra, D.P., Guy, L.K., Park, K.S., and Trimmer, J.S. (2006). Bidirectional activity-dependent regulation of neuronal ion channel phosphorylation. J. Neurosci. *26*, 13505–13514. https://doi.org/10.1523/jneurosci.3970-06.2006.

40. Cocco, L., Follo, M.Y., Manzoli, L., and Suh, P.G. (2015). Phosphoinositide-specific phospholipase C in health and disease. J. Lipid Res. *56*, 1853–1860. https://doi.org/10.1194/jlr.R057984.

41. Heyer, G., Ulmer, F.J., Schmitz, J., and Handwerker, H.O. (1995). Histamine-induced itch and alloknesis (itchy skin) in atopic eczema patients and controls. Acta Derm. Venereol. *75*, 348–352. https://doi.org/10.2340/0001555575348352.

42. Simone, D.A., Alreja, M., and LaMotte, R.H. (1991). Psychophysical studies of the itch sensation and itchy skin ("alloknesis") produced by

intracutaneous injection of histamine. Somatosens. Mot. Res. *8*, 271–279. https://doi.org/10.3109/08990229109144750.

43. Sakai, K., Sanders, K.M., Youssef, M.R., Yanushefski, K.M., Jensen, L., Yosipovitch, G., and Akiyama, T. (2016). Mouse model of imiquimod-induced psoriatic itch. Pain *157*, 2536–2543. https://doi.org/10.1097/j.pain.0000000000000674.
44. Le Pichon, C.E., and Chesler, A.T. (2014). The functional and anatomical dissection of somatosensory subpopulations using mouse genetics. Front. Neuroanat. *8*, 21. https://doi.org/10.3389/fnana.2014.00021.
45. Seal, R.P., Wang, X., Guan, Y., Raja, S.N., Woodbury, C.J., Basbaum, A.I., and Edwards, R.H. (2009). Injury-induced mechanical hypersensitivity requires C-low threshold mechanoreceptors. Nature *462*, 651–655. https://doi.org/10.1038/nature08505.
46. Liu, Q., Sikand, P., Ma, C., Tang, Z., Han, L., Li, Z., Sun, S., LaMotte, R.H., and Dong, X. (2012). Mechanisms of itch evoked by β-alanine. J. Neurosci. *32*, 14532–14537. https://doi.org/10.1523/jneurosci.3509-12.2012.
47. Steele,H.R.,Xing,Y.,Zhu,Y.,Hilley,H.B.,Lawson,K.,Nho,Y.,Niehoff,T.,andHan, L.(2021).MrgprC11(+)sensoryneuronsmediateglabrousskinitch.Proc.Natl. Acad.Sci.USA*118*.https://doi.org/10.1073/pnas.2022874118.
48. Sakai, K., Sanders, K.M., Lin, S.H., Pavlenko, D., Funahashi, H., Lozada, T., Hao, S., Chen, C.C., and Akiyama, T. (2020). Low-threshold mechanosensitive VGLUT3-lineage sensory neurons mediate spinal inhibition of itch by touch. J. Neurosci. *40*, 7688–7701. https://doi.org/10.1523/jneurosci.0091-20.2020.
49. Hill, R.Z., Loud, M.C., Dubin, A.E., Peet, B., and Patapoutian, A. (2022). PIEZO1 transduces mechanical itch in mice. Nature *607*, 104–110. https://doi.org/10.1038/s41586-022-04860-5.
50. Jian, T., Yang, N., Yang, Y., Zhu, C., Yuan, X., Yu, G., Wang, C., Wang, Z., Shi, H., Tang, M., et al. (2016). TRPV1 and PLC participate in histamine H4 receptor-induced itch. Neural Plast. *2016*, 1682972. https://doi.org/10.1155/2016/1682972.
51. Kim, B.M., Lee, S.H., Shim, W.S., and Oh, U. (2004). Histamine-induced Ca(2+) influx via the PLA(2)/lipoxygenase/TRPV1 pathway in rat sensory neurons. Neurosci. Lett. *361*, 159–162. https://doi.org/10.1016/j.neulet.2004.01.019.
52. Than, J.Y.X.L., Li, L., Hasan, R., and Zhang, X. (2013). Excitation and modulation of TRPA1, TRPV1, and TRPM8 channel-expressing sensory neurons by the pruritogen chloroquine. J. Biol. Chem. *288*, 12818–12827. https://doi.org/10.1074/jbc.M113.450072.
53. Li, S., Ding, M., Wu, Y., Xue, S., Ji, Y., Zhang, P., Zhang, Z., Cao, Z., and Zhang, F. (2022). Histamine sensitization of the voltage-gated sodium channel Nav1.7 contributes to histaminergic itch in mice. ACS Chem. Neurosci. *13*, 700–710. https://doi.org/10.1021/acschemneuro.2c00012.
54. Valtcheva, M.V., Davidson, S., Zhao, C., Leitges, M., and Gereau, R.W., 4th. (2015).ProteinkinaseCδmediateshistamine-evokeditchandresponsesinpruriceptors.Mol.Pain*11*,1.https://doi.org/10.1186/1744-8069-11-1.
55. Sharma, N., Flaherty, K., Lezgiyeva, K., Wagner, D.E., Klein, A.M., and Ginty, D.D. (2020). The emergence of transcriptional identity in somatosensory neurons. Nature *577*, 392–398. https://doi.org/10.1038/s41586-019-1900-1.
56. Liu, Q., Tang, Z., Surdenikova, L., Kim, S., Patel, K.N., Kim, A., Ru, F., Guan, Y., Weng, H.J., Geng, Y., et al. (2009). Sensory neuron-specific GPCR Mrgprs are itch receptors mediating chloroquine-induced pruritus. Cell *139*, 1353–1365. https://doi.org/10.1016/j.cell.2009.11.034.

STAR★METHODS

KEY RESOURCES TABLE

REAGENT or RESOURCE	SOURCE	IDENTIFIER
Antibodies		
Chicken polyclonal anti-GFP antibody	Aves Labs	Cat#GFP-1020; RRID: AB_2307313
Rabbit monoclonal (EP2730Y) to PKC (phospho T514)	Abcam	Cat#ab109539; RRID: AB_10863532
Goat polyclonal anti-rabbit IgG H&L Alexa Fluor 488	Abcam	Cat#ab150077; RRID: AB_2630356
Mouse monoclonal anti- GAPDH	Abcam	Cat#ab8245; RRID: AB_2107448
Donkey polyclonal anti-chicken IgY Alexa Fluor 488	Jackson ImmuneResearch	Cat#703-545-155; RRID: AB_2340375
Goat polyclonal anti-mouse IgG, HRP conjugated	Santa Cruz Biotechnology	Cat#sc2005; RRID: AB_631736
Donkey polyclonal anti-rabbit IgG H&L, HRP conjugated	Abcam	Cat#ab205722; RRID: AB_2904602
Chemicals, peptides, and recombinant proteins		
Histamine	Sigma-Aldrich	Cat# H7125
Chloroquine	Sigma-Aldrich	Cat# C6628
Capsaicin	Sigma-Aldrich	Cat# M2028
Tamoxifen	Sigma-Aldrich	Cat# T5648
CNO	Sigma-Aldrich	Cat# C0832
Naltrexone	Sigma-Aldrich	Cat# 1453504
Ibuprofen	Sigma-Aldrich	Cat#I1892
QX-314	Sigma-Aldrich	Cat# 552233
U73122	Sigma-Aldrich	Cat# U6756
Gallein	Tocris Bioscience	Cat# 3090/50
DAPI	Invitrogen	Cat# E140588
Optimal cutting temperature (OCT) compound	SAKURA Tissue-Tek	Cat# 4583
Diphtheria toxin (DTX)	Sigma-Aldrich	Cat#D0564
Resiniferatoxin (RTX)	Tocris Bioscienc	Cat#1137
Dispase	Gibco	Cat# DN25
Collagenase type I	Gibco	Cat#17018029
poly-l-lysine	Sigma-Aldrich	Cat#P8920
Nerve growth factor	Sigma-Aldrich	Cat#N8133
Neurobasal medium	Gibco	Cat#21103049
Fura 2	Invitrogen	Cat#F1201
RIPA lysis and extraction buffer	Thermo Fisher Scientific	Cat#89900
protease inhibitor mix	Thermo Fisher Scientific	Cat#A32965
RNase inhibitor	Life Tech	Cat#4458236
TaqManTM Gene Expression Master Mix	Life Tech	Cat#4369016
B-27 supplement	Gibco	Cat#17504044
L-glutamine	Gibco	Cat#25030081
Western HRP Substrate	Millipore	Cat# WBLUR0100
Critical commercial assays		
RNAscope Multiplex Fluorescent Reagent Kit V2	ACD	Cat # 323100
Single Cell-to-CT TM Kit	Thermo Fisher Scientific	Cat #4458237
Experimental models: Organisms/strains		
Mouse: C57BL/6J	The Jackson Laboratory	JAX: 000664
Mouse: Th^{CreER}	The Jackson Laboratory	JAX: 008532
Mouse: $MrgprD^{CreERT}$	The Jackson Laboratory	JAX: 031286
Mouse: B6N;129-$Tg^{(CAG-CHRM3,\ mCitrine)1Ute/J}$(Gq-DREADD)	The Jackson Laboratory	JAX: 026220

(*Continued on next page*)

Continued

REAGENT or RESOURCE	SOURCE	IDENTIFIER
Mouse: ROSA26^{iDTR}	The Jackson Laboratory	JAX: 007900
Mouse: B6;129S6-Gt (ROSA)26Sor$^{tm9(CAG-tdTomato)Hze}$/J (Ai9)	The Jackson Laboratory	JAX: 007909
Mouse: Piezo2$^{flox/flox}$	The Jackson Laboratory	JAX: 027720
Mouse: Trpa1-KO	The Jackson Laboratory	JAX: 006401
Mouse: PKCδ$^{flox/flox}$	RIKEN BRC	Strain #: 06462
Mouse: Trpv1-EGFP	MMRRC	033029-UCD
Mouse: Trpv1^{Cre}	Mark Hoon, NIH	N/A
Mouse: MrgprA3$^{GFP-Cre}$	Xinzhong Dong, Johns Hopkins University, HHMI	N/A
Oligonucleotides		
RNAscope® Probe- MrgprA3	ACD	Cat #548161
RNAscope® Probe- Piezo2	ACD	Cat #400191
qPCR Taqman probes for Prkca	Thermo Fisher Scientific	Assay ID Mm00440858_m1
qPCR Taqman probes for Prkcb	Thermo Fisher Scientific	Assay ID Mm00435749_m1
qPCR Taqman probes for Prkcd	Thermo Fisher Scientific	Assay ID Mm00440891_m1
qPCR Taqman probes for Prkce	Thermo Fisher Scientific	Assay ID Mm00440894_m1
qPCR Taqman probes for Prkcg	Thermo Fisher Scientific	Assay ID Mm00440861_m1
qPCR Taqman probes for Gapdh	Thermo Fisher Scientific	Assay ID Mm99999915_g1
Software and algorithms		
Prism 9	GraphPad	https://www.graphpad.com/
Adobe Photoshop CS6	Adobe	https://www.adobe.com/
Other		
von Frey filament	North Coast Medical	Cat #NC12775
Piezo Servo Controller	Physik Instrument	E-625

RESOURCE AVAILABILITY

Lead contact

Further information and requests for reagents may be directed to and will be fulfilled by the lead contact, Hongzhen Hu (Hongzhen.Hu@wustl.edu).

Materials availability

This study did not generate new unique reagents.

Data and code availability

All data reported in this paper will be shared by the lead contact upon request.

This paper does not report original code.

Any additional information required to reanalyze the data reported in this work paper is available from the lead contact upon request.

EXPERIMENTAL MODEL AND SUBJECT DETAILS

Animals

All animal procedures were performed using protocols approved by the Animal Studies Committee at Washington University School of Medicine and in compliance with the guidelines provided by the National Institute of Health and the International Association for the Study of Pain. Both adult male and female mice (8–12 weeks old) were used for all experiments and mice were randomly assigned to different experimental conditions. Mice were sex- and age-matched in all experiments and were group-housed in standard mouse housing cages at room temperature with unrestricted access to food and water on a 12 h light/12 h dark cycle.

For lineage tracing, *Ai9* (*B6;129S6-Gt (ROSA)26Sor$^{tm9(CAG-tdTomato)Hze}$/J*) were crossed with *MrgprA3$^{GFP-Cre}$* to induce tdTomato expression in MrgprA3^{+} cells. PCR primers used for genotyping are: Ai9 loxP Forward, CTG TTC CTG TAC GGC ATG G and Ai9

loxP Reverse, GGC ATT AAA GCA GCG TAT CC; Cre Forward, GGTTCGCAAGAACCTGATGG and Cre Reverse, GCCTTCTCTAC ACCTGCGG. The expected product sizes are 196 bps and 550 bps for *Ai9*$^{flox/flox}$ and Cre mice. *Piezo2*$^{flox/flox}$ mice were mated with *Trpv1*^{Cre} and *MrgprA3*$^{GFP\text{-}Cre}$ mice to generate Piezo2 conditional knockout mice (*Piezo2*^{cKO}). PCR primers used for genotyping are: Piezo2 loxP Forward, AGGCTCAGACTTGGAGATCCTGTAGCA and Piezo2 loxP Reverse, GACTCAGATTTTCCACATGG GGGTACTA. The expected product size is 196 bps for *Piezo2*$^{flox/flox}$ mice. *PKCδ*$^{flox/flox}$ mice were mated with *MrgprA3*$^{GFP\text{-}Cre}$ mice to generate PKCδ conditional knockout mice (*PKCδ*^{cKO}). PCR primers used for genotyping are: *PKCδ* loxP Forward, GACAAGATTATCGGCCGCTG and *PKCδ* loxP Reverse, CAAACTGTGGGTTGTCAGAG. The expected product size is 356 bps for *PKCδ*$^{flox/flox}$ mice. The *Rosa26*^{iDTR} mice were crossed with *Trpv1*^{Cre} and *MrgprA3*$^{GFP\text{-}Cre}$mice to obtain *Trpv1*^{Cre}; *iDTR* and *MrgprA3*$^{GFP\text{-}Cre}$; *iDTR* mice. PCR primers used for genotyping are: *DTR* loxP Forward, ATGAAGCTGCTGCCGTCGGTG and *DTR* loxP Reverse, GATCTGCCTCTTGCAAGTCAC. The expected product size is 250 bps for *DTR*$^{flox/flox}$ mice. For chemogenetic activation of DRG neurons, the transgenic mice were engineered by crossing *Trpv1*^{Cre}, *Th*^{CreER}, *MrgprD*^{CreERT} and *MrgprA3*$^{GFP\text{-}Cre}$ mice with *Gq-DREADD (B6N;129-Tg* $^{(CAG\text{-}CHRM3,\ mCitrine)1Ute/J)}$ mice, respectively. PCR primers used for genotyping are: *Gq* loxP Forward, CGCCACCATGTACCCATAC and *Gq* loxP Reverse, GTGGTACCGTCTGGAGAGGA. The expected product size is 204 bps for *Gq*$^{flox/flox}$ mice.

Primary mouse DRG neuronal culture

The DRGs from thoracic and lumbar levels were acutely isolated and cleaned of adhering connective tissue. Isolated ganglia were collected in ice-cold Ca^{2+} and Mg^{2+}-free Hank's buffered salt solution (HBSS, Gibco, USA). DRG neurons were enzymatically digested in dispase (4 U/mL, Gibco, USA) and collagenase type I (342 U/mL, Gibco, USA) dissolved in HBSS for 30 min at 37°C. After digestion, neurons were pelleted, suspended in neurobasal medium containing 2% B-27 supplement, 1% L-glutamine, 100 U·mL^{-1} penicillin plus 100 μg mL^{-1} streptomycin, and 50 ng mL^{-1} nerve growth factor, plated on a 5 mm coverslip coated with poly-l-lysine (10 μg mL^{-1}) and cultured under a humidified atmosphere of 5% CO_2/95% air at 37°C for 18–24 h before use.

METHOD DETAILS

Pruritogen-induced acute chemical itch

To test the acute itch behavior, the fur on the nape of the neck was shaved and mice were acclimated in the red transparent recording chamber for 5 days. On the testing day, mice were habituated in the behavioral testing apparatus for 1 hour and then histamine (50 μg; Sigma-Aldrich, St. Louis MO) or CQ (50 nmol; Sigma-Aldrich, St. Louis, MO) in 30 μL sterile saline was injected intradermally to the nape of the neck. Insulin syringes with 30G needle (UltiCare) were used for intradermal injection. Immediately after the injection, mice were videotaped for 30 min. After the recording, the videotapes were played back and the number of scratch bouts were counted over the 30-min recording period by an investigator blinded to the treatment. A scratching bout is defined as one or more rapid back-and-forth motion of the hindpaw directed to the site of injection, and ending with licking or biting of the toes and/or placement of the hindpaw on the floor.

Pruritogen-induced alloknesis

Mice were acclimated in a red recording chamber with a removable mesh cover for at least 5 days. 30 min after intradermal injection of respective pruritogens, mice received an innocuous mechanical stimulus for 1 second delivered using a von Frey filament (North Coast Medical, bending force: 0.7 mN) at five randomly selected points oriented radially 7 mm away from the injection site. Mice received 3 separate stimulations at each point with an interval of 10 seconds. The scratching response of hind paw toward the poking site was considered as a positive response. The scratching number at each point was averaged and then summed into the final alloknesis score for comparison. The stimulus at 5 points means 5 stimuli.

Drug administration

To induce robust Cre activity, tamoxifen (Sigma-Aldrich) was dissolved in corn oil and made fresh daily before use. Both *Cre*$^{-}$ and *Cre*$^{+}$ mice received intraperitoneal injection of tamoxifen at 100 mg/kg body weight for 5 consecutive days. *In vivo* experiments were performed between 7 and 14 days after tamoxifen injection.

For the chemogenetic stimulation, *Cre*$^{+}$ and *Cre*$^{-}$ *mice* of *Trpv1; Gq-DREADD* mice were intradermally injected with 50 μl 500 nM clozapine N-oxide CNO (Sigma-Aldrich), *Cre*$^{+}$ and *Cre*$^{-}$ *mice* of *Th; Gq-DREADD, MrgprD; Gq-DREADD* and *MrgprA3; Gq-DREADD* mice were intradermally injected with 50 μl 3 mM CNO respectively. Immediately after the injection, mice were videotaped for 60 min. Alloknesis scores were evaluated 0.5 hours after CNO injections.

Mouse cheek model

The right cheek of mice was shaved and acclimated for at least two days before CNO injection. The naltrexone (10 mg/kg) or ibuprofen (150 mg/kg) was injected into each mouse by i.p, 30 minutes later mice were injected intradermally with 20 μL CNO (500 nM) in the right cheek. All mice were videotaped for one hour and the scratching/wiping bouts were counted.

Pharmacological silence of sensory fibers in the skin

Intradermal injection of 30 μL 0.2% QX-314+ 50 nmol CQ are employed to block the the C fibers, respectively. QX-314 (Sigma-Aldrich) and CQ (Sigma-Aldrich) were dissolved in isotonic saline. QX-314 (0.2%, 30 μL) was intradermally injected into the nape of the neck as a vehicle control. The effect of the Phospholipase C (PLC) activator m-3M3FBS (20 μM, 30 μL; Sigma-Aldrich), PLC antagonist U73122 (0.1 μM, 30 μL; Sigma-Aldrich) and the G protein βγ subunit inhibitor gallein (500 μM, 30 μL; Tocris Bioscience) and on scratching and alloknesis was tested.

In situ hybridization and immunohistochemistry

Non-isotopic *in situ* hybridization (ISH) on DRG sections prepared from *MrgprA3*$^{GFP\text{-}Cre}$ and *Trpv1-EGFP* mice were performed to detect Piezo2 mRNA expression. RNAscope Multiplex Fluorescent Reagent Kit V2 (Cat # 323100) and Piezo2 probes (400191) were purchased from ACDBio. The ISH/GFP double staining was performed as previously described.[56] Briefly, after *in situ* hybridization for Piezo2 as instructed in the manual, DRG sections were incubated overnight at 4°C with chicken anti-GFP antibody (GFP-1020, Aves Labs, 1:1,000) and then incubated for 1 h at room temperature with donkey anti-chicken IgY (703-545-155, Alexa Fluor 488 conjugated, Jackson ImmuneResearch). Sections were then washed three times in PBS and mounted with DAPI for imaging.

To detect pruritogen-induced p-PKC expression in the MrgprA3$^+$ neurons, wt mice were divided into eight groups for double staining. Four groups of mice were intradermally injected with vehicle (isotonic saline), CQ (50 nmol, 30 μL), U73122 (0.1 μM, 30 μL; 30 min prior to the CQ) + CQ and gallein (500 μM, 30 μL; 30 min prior to the CQ) + CQ respectively, and the other four groups were administered intradermally with vehicle (isotonic saline), histamine (50 μg, 30 μL), U73122 (0.1 μM, 30 μL; 30 min prior to the histamine) + histamine and gallein (500 μM, 30 μL; 30 min prior to the histamine) + histamine respectively. Thirty minutes after treatments, mice were deeply anesthetized with 2% isoflurane and were perfused intracardially with phosphate buffered saline (PBS, 0.1 M, pH 7.4) followed with fixative (4% paraformaldehyde, pH 7.4) at room temperature. Thoracic DRG were dissociated and fixed in fixative at 4°C for overnight, then stored in 30% sucrose in PBS at 4°C for 3 days. Samples were then embedded in optimal cutting temperature (OCT) compound (Sakura Finetek, Tissue-Tek, PA). Sections of approximately 12 μm on slides were performed for ISH with MrgprA3 probes (548161, ACDBio) firstly, then DRG sections were incubated overnight at 4°C with rabbit antibody to p-PKC (ab109539, Abcam, 1:500) and then incubated for 1 h at room temperature with goat anti-rabbit IgG H&L (ab150077, Alexa Fluor® 488, Abcam).

Both fluorescent and ISH signals were observed under the Nikon C2 Confocal Laser Microscope. Only DRG cells with clearly visible nuclei were quantified to prevent double-counting of the same cells in different sections. For quantification, 3–5 DRG sections from 3 mice were analyzed in each group.

Tail flick test

The ablation efficiency of the TRPV1$^+$ neurons were determined by the tail flick test. The tail flick response to 51°C hot water was recorded. 20 s was set as the cut-off time.

Chemical ablation of TRPV1$^+$ and MrgprA3$^+$ neurons

For systemic DTX-mediated cell ablation, *Trpv1*^{Cre}; *iDTR* and *MrgprA3*$^{GFP\text{-}Cre}$*; iDTR* mice were treated with diphtheria toxin (DTX), according to the previous methods with a little modification.[8] Briefly, 6 weeks old mice were injected intraperitoneally with DTX (50 mg/kg; Sigma-Aldrich) in 100 μL PBS at day 1, day 4, day7 and day 10. Mice were allowed for four weeks rest before behavioral experiments. For chemical ablation of Trpv1$^+$ neurons, C57BL/6 mice at 4 weeks of age were treated with resiniferatoxin (RTX, Tocris Bioscience). RTX was prepared in 2% DMSO with 0.15% Tween 80 in PBS. Mice received subcutaneous injections of RTX in the flank on consecutive days with three increasing doses of RTX (30, 70, and 100 μg/kg). We performed behavioral experiments 4 to 6 weeks after RTX injection. Considering the potential variation of ablation efficiency in different approaches, mice displayed significantly increased latency to thermal pain response and less than 5% capsaicin-responding DRG neurons were kept for further analysis.

Mouse DRG neuron cultures

Mice were deeply anaesthetized with isoflurane and then exsanguinated. The spinal cord was removed and DRG from thoracic levels were dissected. Isolated ganglia were collected in ice-cold Ca^{2+} and Mg^{2+}-free Hank's buffered salt solution (HBSS, Gibco). DRG neurons were enzymatically digested in dispase (4 U/mL, Gibco) and collagenase type I (342 U/mL, Gibco) dissolved in HBSS for 30 min at 37°C. After digestion, neurons were pelleted, suspended in neurobasal medium containing 2% B-27 supplement, 1% L-glutamine, 100 U·mL^{-1} penicillin plus 100 μg mL^{-1} streptomycin, and 50 ng mL^{-1} nerve growth factor, plated on a 5 mm coverslip coated with poly-l-lysine (10 μg mL^{-1}) and cultured under a humidified atmosphere of 5% CO_2/95% air at 37°C for 18–24 h before use.

Live-cell calcium imaging

Culture DRG neurons on cover slips were loaded with 4 μmol/L fura 2 (Invitrogen) for 60 min in the dark at 37°C. After a three-time wash with HBSS, the cells were imaged by a microscope. Fluorescence at 340 and 380 nm excitation wavelengths was recorded on an inverted Nikon Ti-E microscope equipped with 340, 360 and 380 nm excitation filter wheels using NIS-Elements imaging software (Nikon Instruments Inc., Melville, NY, USA). Fura-2 ratios (F340/F380) were used to reflect changes in intracellular Ca^{2+} upon stimulation. Values were obtained from 80 to 150 cells in time-lapse images from each coverslip. The standard extracellular solution for

Ca^{2+} imaging in cultured DRG neurons contained 140 mM NaCl, 5 mM KCl, 2 mM $CaCl_2$, 2 mM $MgCl_2$, 10 mM Na-HEPES, and 10 mM glucose (pH 7.3). Chloroquine (1 μM), capsaicin (300 nM) and KCl (100 mM) was dissolved respectively in standard extracellular solution.

Dissociated DRG neurons from *Trpv1*^{Cre} and *Trpv1*^{Cre};*Piezo2*$^{flox/flox}$ mice were first screened for capsaicin sensitivity using calcium imaging to pick up the TRPV1$^+$ neurons, and then labeled for following patch clamp recordings.

Whole-cell patch-clamp recordings

Whole-cell patch-clamp recordings were performed using a Multiclamp 700B amplifier (Molecular Devices, Sunnyvale, CA, USA) at room temperature (22–24°C) on the stage of an inverted phasecontrast microscope equipped with a filter set for tdTomato visualization. Pipettes pulled from borosilicate glass (BF 150-86-10; Sutter Instrument Company, Novato, CA, USA) with a Sutter P-1000 pipette puller had resistances of 2–4 MΩ when filled with pipette solution containing 120 mM K^+-gluconate, 30 mM KCl, 2 mM $MgCl_2$, 1 mM $CaCl_2$, 2 mM MgATP, 11 mM EGTA, and 10 mM HEPES with pH 7.3. Cells were continuously perfused with standard extracellular solution containing 145 mM NaCl, 3 mM KCl, 2 mM $CaCl_2$, 2 mM $MgCl_2$, 10 mM glucose and 10 mM HEPES (pH was adjusted to 7.4 with NaOH). Cells were clamped to a holding potential of −80 mV and stimulated with a series of mechanical stimuli in 1 μm increments every 10 s, and the stimulus was applied for 100 ms. Step indentations were applied using a fire-polished glass pipette (tip diameter 2–3 μm) that was positioned at an angle of 70° to the surface of the cell. The pipette was controlled by a Piezo Servo Controller (E-625, Physik Instrument, Karlsruhe, Germany). Data were acquired using pClampex 10 (Molecular Devices, San Jose, CA). Currents were filtered at 2 kHz and digitized at 10 kHz. Values were given as mean ± SEM; n represents the number of measurements.

Western blot analysis

DRG isolated from thoracic levels were homogenized in ice-cold RIPA lysis and extraction buffer (Thermo Fisher Scientific) with protease inhibitor mix (Thermo Fisher Scientific). Proteins were separated by SDS-PAGE gel electrophoresis and transferred to a PVDF membrane (Millipore Corp) which was blocked for 1 h at room temperature. The membrane was then incubated overnight at 4°C with monoclonal antibody against p-PKC (ab109539, Abcam, 1:1000) and as loading control antibody against GAPDH (ab8245, Abcam, 1:1000). Subsequently, PVDF membranes were incubated with goat anti-mouse IgG (sc2005, Santa Cruz Biotechnology, 1:3000) or donkey-anti-rabbit IgG H&L (ab205722, Abcam, 1:3000).

Single cell RT-PCR

To isolate MrgprA3$^+$ neurons, DRGs from *MrgprA3*^{Cre};*Ai9*$^{f/f}$ mice were dissected and dissociated. DRG neurons were purified using a 15% BSA density gradient column. MrgprA3$^+$ neuron cells were visually identified under a Nikon eclipse TE2000-S microscope and manually picked using a Sutter Instrument ROE285-4323 micromanipulator. Isolated MrgprA3$^+$ neurons were ejected into PCR tubes containing 10 μL of lysis buffer and RNase inhibitor (4458236, Life Tech), and flash frozen on dry ice and stored at −80°C until cDNA synthesis.

cDNA was generated using Invitrogen Single Cell-to-CT TM Kit (4458236, Life Tech), according to the manufacturer's protocol. RT-PCR was performed using 2 μL cDNA and TaqManTM Gene Expression Master Mix(4369016, Life Tech). qPCR Taqman probes (Thermo Fisher Scientific) used were Prkca: Assay ID Mm00440858_m1; Prkcb: Assay ID Mm00435749_m1, Prkcd: Assay ID Mm00440891_m1, Prkce: Assay ID Mm00440894_m1, Prkcg: Assay ID Mm00440861_m1 and Gapdh: Assay ID Mm99999915_g1. PCR reactions were run in triplicate.

QUANTIFICATION AND STATISTICAL ANALYSIS

Results are expressed as mean ± SEM. All histology, calcium imaging, and electrophysiology experiments were repeated using tissues from at least three different mice. Statistical analysis was performed in Prism 9 (GraphPad). A threshold of $p < 0.05$ was accepted as statistically different and $p > 0.05$ considered non-significant. For itch behavioral test, we did not observe any obvious sex differences in our experiments and data from both genders were pooled together for futher analysis with unpaired two-tailed Student's *t* test (for two groups) or one-way ANOVA (for three or more groups). For statistical analysis of incidence of electrophysiological results, data were analyzed with Chi-square test.

Cell Reports, Volume *42*

Supplemental information

MrgprA3-expressing pruriceptors drive pruritogen-induced alloknesis through mechanosensitive Piezo2 channel

Ping Lu, Yonghui Zhao, Zili Xie, Huan Zhou, Xinzhong Dong, Gregory F. Wu, Brian S. Kim, Jing Feng, and Hongzhen Hu

SUPPLEMENTAL INFORMATION

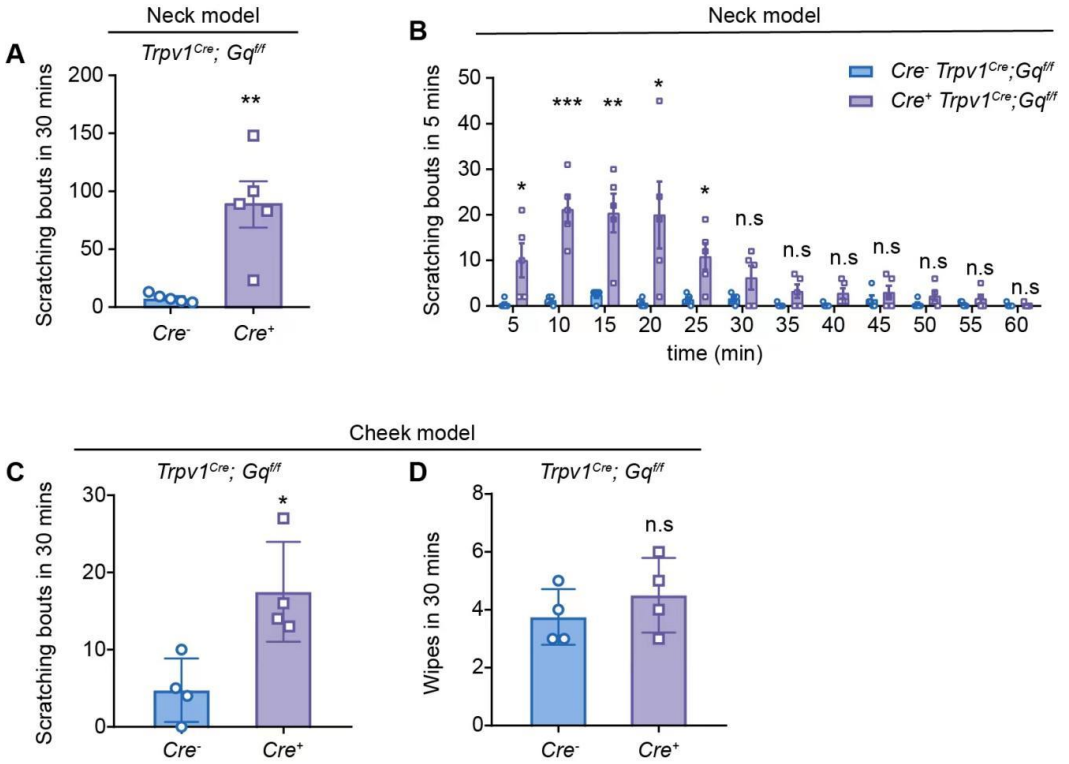

Supplementary Figure 1. Chemogenetic activation of TRPV1$^+$ neurons evokes spontaneous scratching in *Trpv1-hM3Dq* mice. **A**, CNO-induced spontaneous scratching response in *Cre*$^-$ and *Cre*$^+$ *Trpv1-hM3Dq* mice. n=5 for each group. **B**, Time course of CNO-induced spontaneous scratching at 5-min intervals over 60 mins. n=5 for each group. **C-D,** CNO-induced scratching (**C**) and wiping (**D**) responses in the cheek model. The total numbers were counted over the first 30 mins after i.d. injection of CNO in the *Cre*$^-$ and *Cre*$^+$ *Trpv1-hM3Dq* mice. n=4 for each group. All data are expressed as mean ± SEM. n.s, not significant, **P*<0.05, ***P*<0.01, ****P*<0.001. Unpaired two-tailed Student's t test.

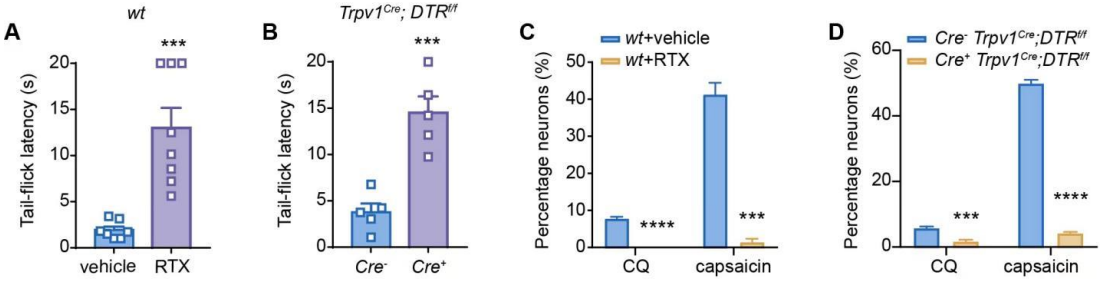

Supplementary Figure 2. Validation of RTX-induced TRPV1$^+$ neuron ablation. **A,** Tail-flick latency of *wt* mice treated with vehicle (n=7) or RTX (n=8). **B**, Tail-flick latency of *Cre*$^-$ (n=5) and *Cre*$^+$ (n=5) *Trpv1*^{Cre}; *DTR*$^{f/f}$ mice treated with DTX. **C** and **D**, Percentage of DRG neurons responding to CQ and Capsaicin in calcium imaging assays. In DRG cultures from RTX-treated *wt* mice there were no CQ-sensitive neurons and only 1.4±0.9% neurons responding to capsaicin while there were 7.8±0.5% neurons responding to CQ and 41.3±3.1% neurons were sensitive to capsaicin in DRG cultures from vehicle-treated *wt* mice (**C**). In DRG cultures from DTX-treated *Cre*$^+$ *Trpv1*^{Cre}; *DTR*$^{f/f}$ mice, there were 1.7±0.5% neurons responding to CQ and 4.2±0.4% neurons responding to capsaicin while there were 5.8±0.5% neurons responding to CQ and 49.9 ± 1.1% neurons responding to capsaicin in DRG cultures from DTX-treated *Cre*$^-$ *Trpv1*^{Cre}; *DTR*$^{f/f}$ mice (**D**). All data are expressed as mean ± SEM. ***P<0.001, ****P<0.0001, Unpaired two-tailed Student's t test.

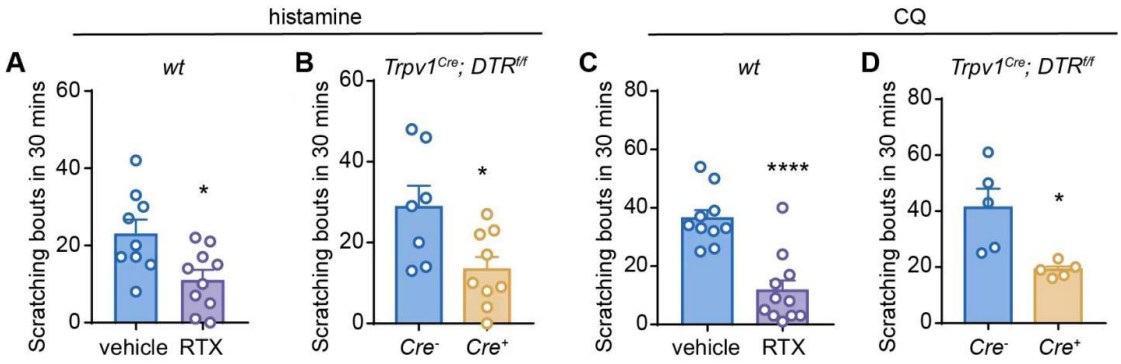

Supplementary Figure 3. Ablation of TRPV1$^+$ neurons attenuates pruritogen-induced acute chemical itch. A, Histamine-induced acute chemical itch response in RTX-treated (n=10) and vehicle-treated (n=9) *wt* mice. **B**, Histamine-induced acute chemical itch response in *Cre*$^-$ (n=7) and *Cre*$^+$ (n=9) *Trpv1-DTR* mice treated with DTX. **C**, CQ-induced acute chemical itch response in RTX-treated (n=11) and vehicle-treated *wt* mice (n=10). **D**, CQ-induced acute chemical itch response in *Cre*$^-$ (n=5) and *Cre*$^+$ (n=5) *Trpv1-DTR* mice treated with DTX. All data are expressed as mean ± SEM.**P*<0.05, *****P*<0.0001. Unpaired two-tailed Student's t test.

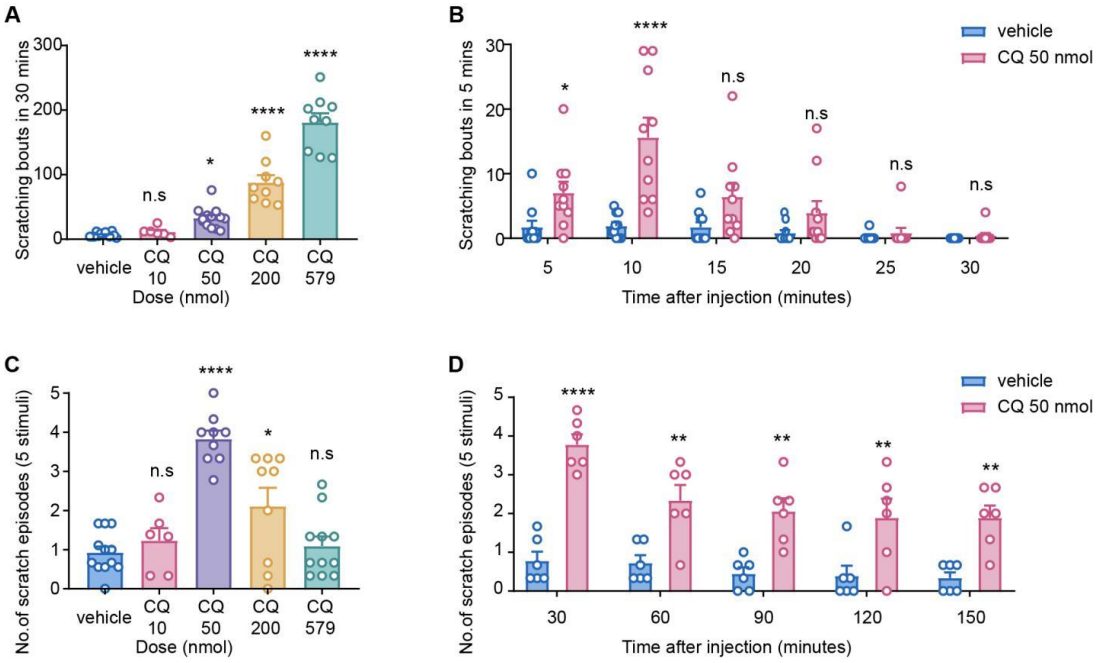

Supplementary Figure 4. Characterization of CQ-induced mechanical itch in *wt* mice. A, Dose dependency of acute chemical itch response evoked by CQ. **B,** Time course of 50 nmol CQ-induced acute chemical itch response. **C**, Dose dependency of CQ-induced mechanical itch response. **D**, Time course of 50 nmol CQ-induced mechanical itch response. All data are expressed as mean ± SEM. n.s, not significant. **P*<0.05, ***P*<0.01, *****P*<0.0001. One way ANOVA in A and C and unpaired two-tailed Student's t test in B and D.

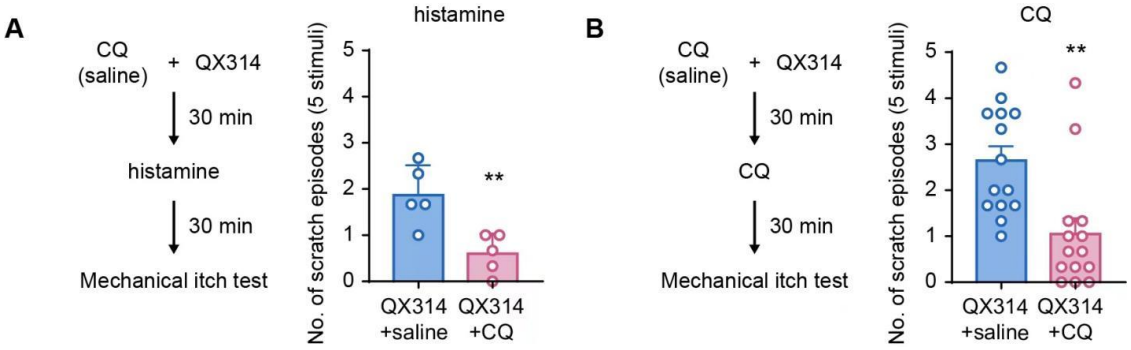

Supplementary Figure 5. QX314-induced silencing of TRPV1$^+$ neurons attenuates pruritogen-induced mechanical itch. A, Histamine-induced mechanical itch response in mice treated with QX314 + saline or QX314 + CQ. n=5 for each group. **B**, CQ-induced mechanical itch response in mice treated with QX314 + saline or QX314 + CQ. n=14 for each group in B. All data are expressed as mean ± SEM. n.s, not significant. ***P*<0.01. Unpaired two-tailed Student's t test.

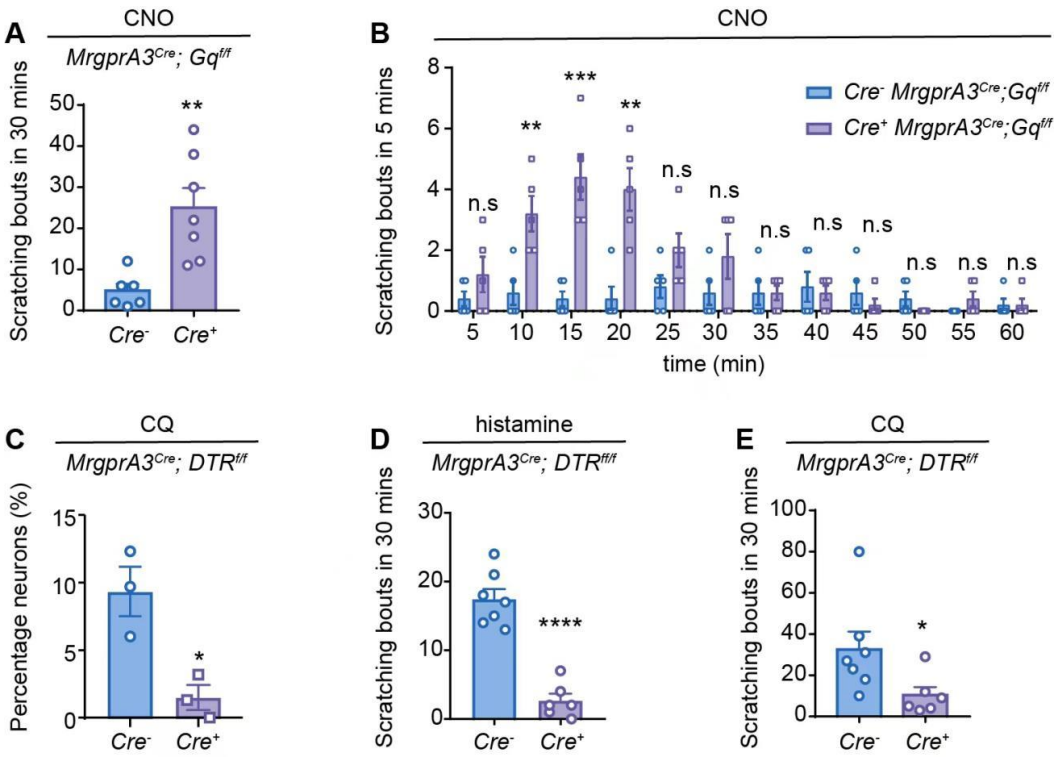

Supplementary Figure 6. MrgprA3$^+$ neurons are critically involved in acute chemical itch. **A,** CNO-evoked spontaneous scratching in *Cre*$^-$ (n=6) and *Cre*$^+$ (n=7) *MrgprA3-hM3Dq* mice. **B**, Time course of CNO-induced spontaneous scratching at 5-min intervals over 60 minutes. n=5 for each group. **C**, Percentage of CQ-responding DRG neurons isolated from DTX-treated *Cre*$^-$ (n=3) or *Cre*$^+$ (n=3) *MrgprA3-DTR* mice. **D**, Histamine-evoked spontaneous scratching in the DTX-treated *Cre*$^-$ (n=7) and *Cre*$^+$ (n=6) *MrgprA3-DTR* mice. **E**, CQ-evoked spontaneous scratching in DTX-treated *Cre*$^-$ (n=7) and *Cre*$^+$ (n=6) *MrgprA3-DTR* mice. All data are expressed as mean ± SEM. n.s, not significant. **P*<0.05, ***P*<0.01, ****P*<0.001, *****P*<0.0001. Unpaired two-tailed Student's t test.

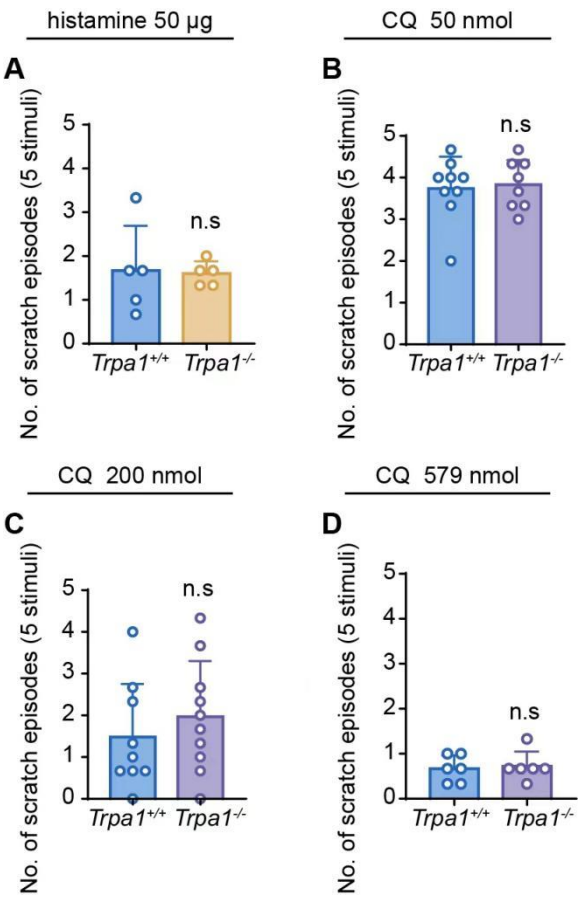

Supplementary Figure 7. TRPA1 is not required for histamine- and CQ-induced mechanical itch. A, Histamine-induced alloknesis scores in *Trpa1*$^{+/+}$ (n=5) and *Trpa1*$^{-/-}$ mice (n=5). **B** to **D**, CQ-induced alloknesis scores in *Trpa1*$^{+/+}$ and *Trpa1*$^{-/-}$ mice at different doses. For 50 nmol CQ treatment, n=9 in *Trpa1*$^{+/+}$ group, n=8 in *Trpa1*$^{-/-}$ group; For 200 nmol CQ treatment, n=9 in *Trpa1*$^{+/+}$ group, n=10 in *Trpa1*$^{-/-}$ group; For 579 nmol CQ treatment, n=6 in each group. All data are expressed as mean ± SEM. n.s, not significant. Unpaired two-tailed Student's t test.

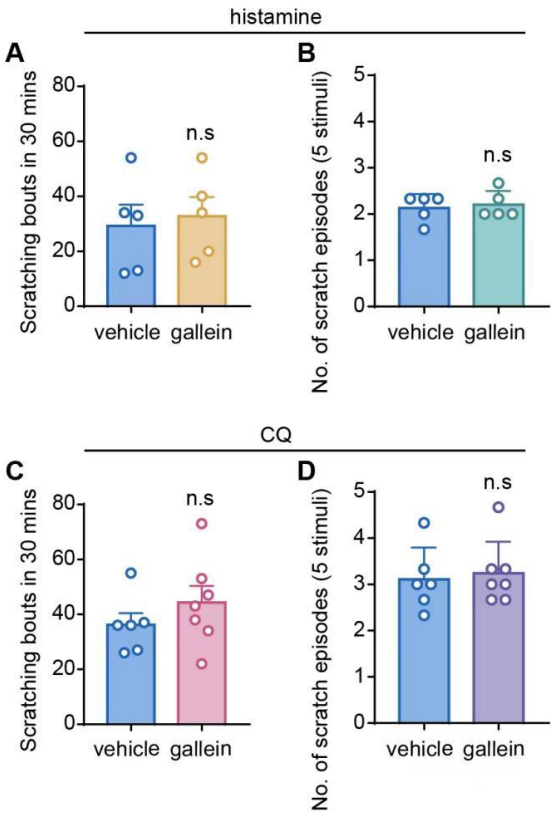

Supplementary Figure 8. Pharmacological inhibition of Gβγ signaling does not affect pruritogen-induced acute chemical itch or mechanical itch. A-B, Histamine-induced acute chemical itch (**A**) and mechanical itch (**B**) in vehicle-treated (n=5) and gallein-treated (n=5) *wt* mice. **C-D**, CQ-induced acute chemical itch (**C**) and mechanical itch (**D**) in the vehicle-treated (n=6) and gallein-treated (n=7) *wt* mice. All data are expressed as mean ± SEM. n.s, not significant. Unpaired two-tailed Student's t test.

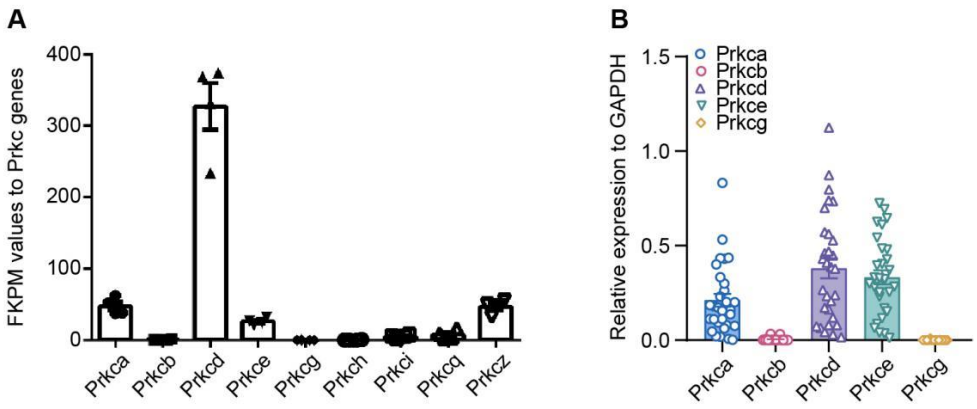

Supplementary Figure 9. Expression levels of PKC genes in MrgprA3$^+$ neurons. **A**, Published data from Yanyan Xing et al (Supplementary Table S5 in the original paper). Normalized expression levels were reported as fragments per kilobase of transcript per million mapped reads (FPKM). **B**, Single-cell qRT-PCR assay detected mRNA expression of PKC isoform genes in MrgprA3$^+$ neurons.

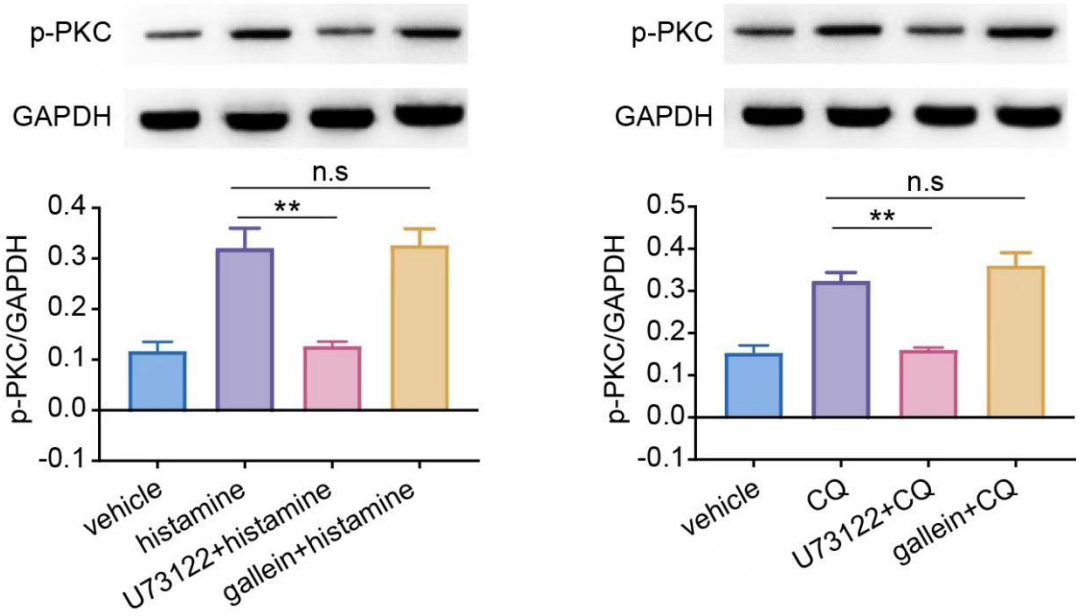

Supplementary Figure 10. Pruritogen-induced p-PKC protein expression is dependent on PLC signaling. Top**,** representative Western Blot data obtained from DRG lysates subjected to different treatments using antibodies against phosphorylated PKC (p-PKC) and GAPDH. Bar charts illustrate the quantification of p-PKC expression in DRG lysates. Data are expressed as mean ± SEM. n=3 for each group. n.s, not significant, ***P*<0.01, Unpaired two-tailed Student's t test.

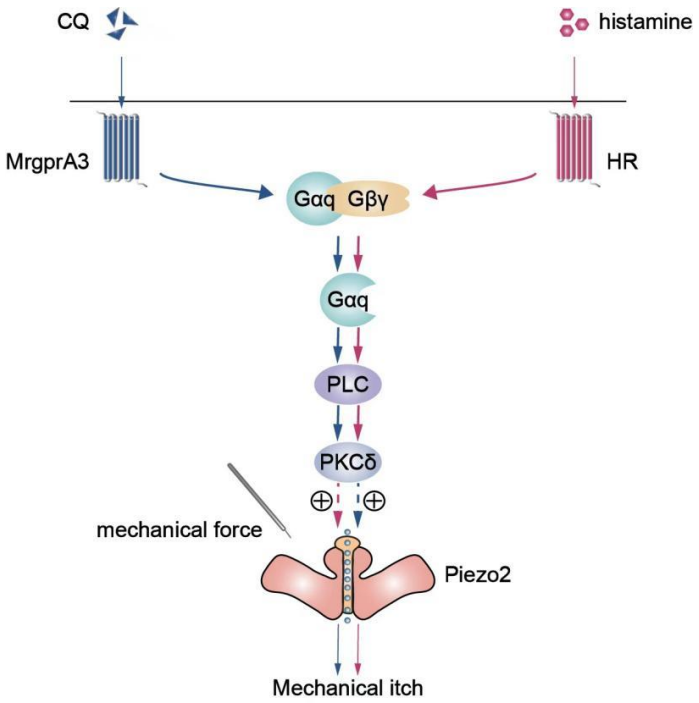

Supplementary Figure 11. Schematic diagram illustrating the signaling pathway in pruritogen-induced alloknesis. CQ and histamine activate MrgprA3 and histamine receptors respectively, which causes dissociation of $G_{\alpha q}$ and drives downstream PLC/PKCδ signaling, resulting in sensitization of pruriceptor-expressing Piezo2 channel and subsequently promoting alloknesis.